ELECTROCHEMSENSE: ELECTROCHEMICAL REAL-TIME

PESTICIDE SENSING SYSTEM

by

Vikram Narayanan Dhamu

APPROVED BY SUPERVISORY COMMITTEE:

_____

Dr. Shalini Prasad, Chair

_____

Dr. Fang Bian

_____

Dr. Shashank Sirsi

ELECTROCHEMSENSE: ELECTROCHEMICAL REAL-TIME PESTICIDE SENSING SYSTEM

by

VIKRAM NARAYANAN DHAMU, BE

THESIS

Presented to the Faculty of

The University of Texas at Dallas

in Partial Fulfillment

of the Requirements

for the Degree of

MASTER OF SCIENCE IN

BIOMEDICAL ENGINEERING

THE UNIVERSITY OF TEXAS AT DALLAS

May 2019

ACKNOWLEDGMENTS

To start off, I would like to take this opportunity to thank Dr. Shalini Prasad, first for simply being my teacher who has taught me so much these last 2 years. Next, for considering me to be a part of the Biomedical Microdevices and Nanotechnology Laboratory (BMNL)-UTD and being patient with me through my mistakes and guiding me through the whole master's program.

A big thanks to my thesis committee members- Dr. Fang Bian and Dr. Shashank Sirsi- for their timely advice and feedback to improve ElectrochemSENSE.

A special thank you to Devangsingh Sankhala, Badrinath Jagannath and Alejandro Abraham for being part of this thesis study and the many late nights of work. I also thank all my other colleagues at BMNL, for their constant support.

The biggest thank you to my family and friends, for their unflinching support and sacrifice for me to get to the point where I am today. Lastly, thank you God for being by my side and keeping faith in me through the ups and downs.

April 2019

ELECTROCHEMSENSE: ELECTROCHEMICAL REAL-TIME

PESTICIDE SENSING SYSTEM

Vikram Narayanan Dhamu, MS
The University of Texas at Dallas, 2019

Supervising Professor: Dr. Shalini Prasad

Pesticide contamination of produce and water in the United States has been a drastic problem to address partly due to the high overhead costs of screening in produce samples, while the other being the inability to report data in real-time-accurately. In 2007, Glyphosate was the most widely used pesticide in the US agricultural sector. More recently, the use of Glyphosate-based herbicides (GBH) has been reported to have increased more than 100-fold with the emergence of glyphosate resistant weeds. The WHO has classified it as being possibly carcinogenic to humans with more current reports suggesting that a few days of GBH use per year-increases the risk of cancer two-fold. In addition to this, it has been known to cause chromosomal damage to cells. But, while there is high interest and a necessity to detect this compound-the challenge however lies in designing a sensitive, low volume sensor that can screen for glyphosate with high specificity directly from produce run-off/extract and report it as useful concentration information. In this study, we have developed a portable real-time electrochemical sensing system that can identify and report trace levels of Glyphosate as below or above the Maximum Residue Limit (MRL) of that particular produce type. Through an optimized label-free assay protocol developed in our laboratory, we

have built and characterized an electrochemical sensor device that utilizes Chronoamperometry as the detection modality to characterize concentration of glyphosate pesticide as a measure of current-It gauges the chemical interactions occurring at the active sensing region to modulations in electrical signal response. Using this system makes it possible to detect concentrations as low as 0.01ppm (1ng/mL), which is the sensor's limit of detection (LOD). The device currently in the form factor of a small box can report contaminant concentration of glyphosate in the produce sample in under a minute (rapid) using a GREEN or RED light for SAFE (low) or UNSAFE (high) threshold ranges based on MRL/residue tolerance values of the produce in question. Hence, we have built an effective, low-cost, portable tool eliminating time consuming laboratory analysis that can be used by consumers and industry alike to keep a check on food safety and quality.

TABLE OF CONTENTS

LIST OF FIGURES

LIST OF TABLES

CHAPTER 1

INTRODUCTION

1.1 Project Objective and Goal

The overall objective of this research is to build an Electrochemical Real-time Pesticide Sensing System that can screen for glyphosate in produce run-off/extract and report whether it is safe or unsafe to consume (i.e. contaminated with glyphosate or not).

For this application, we have 3 specific aims to design and characterize the sensing system as given below:

Specific Aim 1:

Electrochemical Sensor characterization and feasibility study

The first aim deals with designing and characterizing an electrode system and determine whether it is feasible to implement in an electrochemical sensing application. Different electrode designs and substrates were considered to obtain best sensor performance. Also, optimal fluid volume and electrode dimensions are inferred in this aim. Finally, the electrochemical immunoassay and chemistry is constructed and further validated to prove overall sensor feasibility.

Specific Aim 2a:

Study of Electrochemical Sensor Response in various Samples tested on Gamry Lab Instrument.

This particular specific aim is recognized as the experimental protocol validation step, wherein the sensor performance is tested using a laboratory benchtop instrument-Gamry Potentiostat and results obtained initially to monitor/detect Glyphosate levels in a synthetic buffer medium-Phosphate Buffer Saline (PBS) and improve the protocol accordingly based on which to further detect Glyphosate Pesticide in various produce run off/extract solutions. Here, the laboratory

instrument acts as the gold standard to determine whether or not the sensing mechanism is viable.

Specific Aim 2b:

Study of Electrochemical Sensor Response in various Samples tested on Pesticide Reader device

From the results obtained in the previous aim, the optimized experimental immunoassay protocol is implemented using a field reader device designed specifically for this application and the sensor performance results are recorded similar to that of the previous step-initially to detect glyphosate pesticide levels in a synthetic buffer medium (PBS) and subsequently in produce run-off/extract sample solutions.

Specific Aim 3a:

Comparing performances of Lab Instrument and Pesticide Reader

Once the performances on both- the standard laboratory instrument as well as the field reader device is recorded, the results are plotted together to determine how they measure against one another in terms of resolution and accuracy.

Specific Aim 3b:

Cross-Reactivity Study to determine Glyphosate Specificity

It is highly crucial that the developed sensing mechanism can accurately detect glyphosate levels in the samples with high specificity, this specific aim deals in particular to experimentally depict that the sensor is capable of being specific to glyphosate by comparing its dose response with that of a related pesticide-Glufosinate.

Specific Aim 3c:

Machine Learning Classifier Integration

In this aim, a proof of concept is developed for integrating machine learning functionality to the sensing system so that sensor response prediction can be characterized to perform with high accuracy and also serve as an analytics medium thereby minimizing error rate.

1.2 Background

Glyphosate is an organophosphorus herbicide that is applied to the leaves of plants and crops to kill broadleaf plants and grasses. It is known to be a non-selective herbicide, which implies it will kill most weed types. Glyphosate was first used in USA in the year 1974. It is now the most widely used pesticide in the country for agricultural use and also finds application to remove weeds in the Industrial area while in some products it is utilized to control aquatic plants. Currently, there are more than 750 glyphosate based products for sale in the United States.[37]

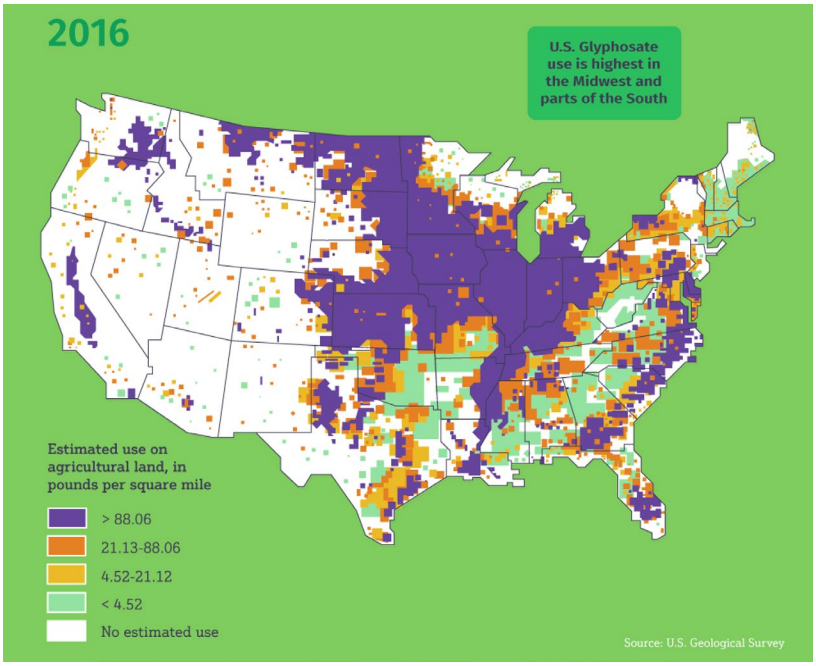

Figure 1.1: Estimated use of Glyphosate in the United States for the year 2016[48]

Active Ingredient	Type	2012		2009		2007*		2005*	
		Rank	Range	Rank	Range	Rank	Range	Rank	Range
Glyphosate	H	1	270-290	1	209-229	1	170-190	1	147-167
Atrazine	H	2	64-74	2	59-69	2	70-80	2	66-76
Metolachlor-S	H	3	34-44	6	24-34	4	27-37	5	25-35
Dichloropropene	Fum	4	32-42	4	27-37	6	24-34	4	28-38
2,4-D	H	5	30-40	5	24-34	7	22-32	7	21-31
Metam	Fum	6	30-40	3	30-40	3	48-58	3	36-46
Acetochlor	H	7	28-38	7	23-33	5	25-35	6	24-34
Metam Potassium	Fum	8	16-26	8	14-24	13	6-10	—	0-3
Chloropicrin	Fum	9	8-18	9	6-16	9	5-15	10	5-15
Chlorothalonil	F	10	6-16	11	6-10	12	6-10	13	6-10
Pendimethalin	H	11	6-16	10	6-16	10	6-10	9	5-15
Ethephon	PGR	12	7-11	12	6-10	11	6-10	11	7-11
Mancozeb	F	13	5-9	16	3-7	19	3-7	16	5-9
Chlorpyrifos	I	14	4-8	13	5-9	14	6-10	15	5-9
Metolachlor	H	15	4-8	22	1-5	—	0-4	—	0-3
Hydrated Lime	F	16	3-7	15	4-8	20	2-6	—	1-5
Propanil	H	17	3-7	17	3-7	18	3-7	18	3-7
Dicamba	H	18	3-7	25	1-5	—	1-5	22	1-5
Trifluralin	H	19	3-7	18	3-7	17	4-8	14	6-10
Decan-1-ol	PGR	20	3-7	—	1-5	—	1-5	—	0-4
Copper Hydroxide	F	21	3-7	20	2-6	15	5-9	12	7-11
Acephate	I	22	2-6	—	1-5	22	1-5	23	1-5
Paraquat	H	23	2-6	—	1-5	25	1-5	24	1-5
Methyl Bromide	Fum	24	2-6	14	5-9	8	8-18	8	9-19
Glufosinate	H	25	2-6	—	1-5	—	1-5	—	0-4

Figure 1.2: Table emphasizing the wide use of Glyphosate in USA[49]

According to various reports[25][36], Global market for glyphosate was valued at 7.24 Billion USD and is expected to increase to reach 10.88 Billion USD by the year 2024. In terms of volume usage, 785.30 kilotons of glyphosate use was estimated for the year 2017.

Asia Pacific was the biggest market for glyphosate in the past decade, the reason being the abundant availability of arable land in the region with china being one of the major producers and consumer in the world with high capacity to produce and export glyphosate across the globe. Next, Latin America, North America and Europe are considered important outlets for glyphosate market with the shifting trend in agriculture towards genetically modified (GM) crops based farming in countries like Germany and UK. Also, Countries in Middle East and Africa are expected to achieve moderate-sustainable growth in market share and use over the forthcoming years. Figure 1.2 depicts the use of organophosphate based herbicides globally based on a study conducted by the Environmental Protection Agency (EPA).

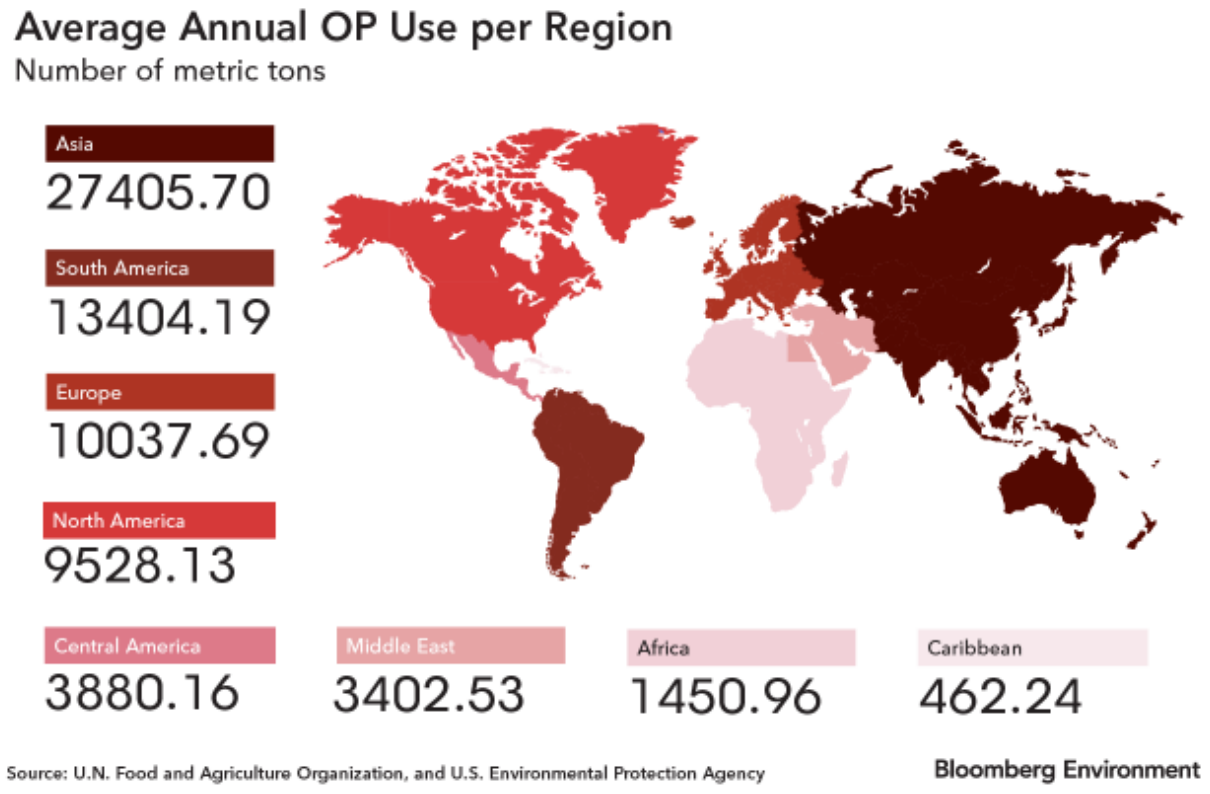

Figure 1.3: Global use of Organophosphate (OP) based herbicides (based on data from 2016)[38]

1.3 Health Impacts associated with glyphosate

A report from the World Health Organization's International Agency for Research on Cancer (IARC) concluded that glyphosate was 'probably carcinogenic' after a consolidated review of scientific journal papers and peer-review publications. This was followed by the U.S. Environmental Protection Agency (EPA) going back and forth on their draft report that glyphosate is unlikely to pose a cancer risk to humans. The research [7] [17] [19] [20] around this glyphosate has become highly politicized and controversial. Environmental activists claim exposure and contaminated produce intake is linked to a wide spectrum of diseases including cancer [16], reproductive issues, neural disorders, and etc. while on the other hand, industry-backed reviews and certain regulatory institutions continue to emphasize that no effects concerning impacts on health has been proven.

Figure 1.4: Acceptable daily intake for humans based on body weight (kg)[21]

However, there is some research which hypothesize that glyphosate behaves as an endocrine disruptor [14] based of experiments on human liver HepG2 cells exposed to different formulations of glyphosate based herbicides. It showed effects of estrogen hormone receptor inhibition as well cytotoxic and DNA damage problems. Similarly, certain studies have revealed

the association of non-alcoholic fatty liver disease [15] in rats after exposure to low doses of glyphosate formulations. Other effects to glyphosate like adverse outcomes on pregnancy [13] (reproductive issues), birth defects, and celiac disease [18] have also been studied and published in the scientific community.

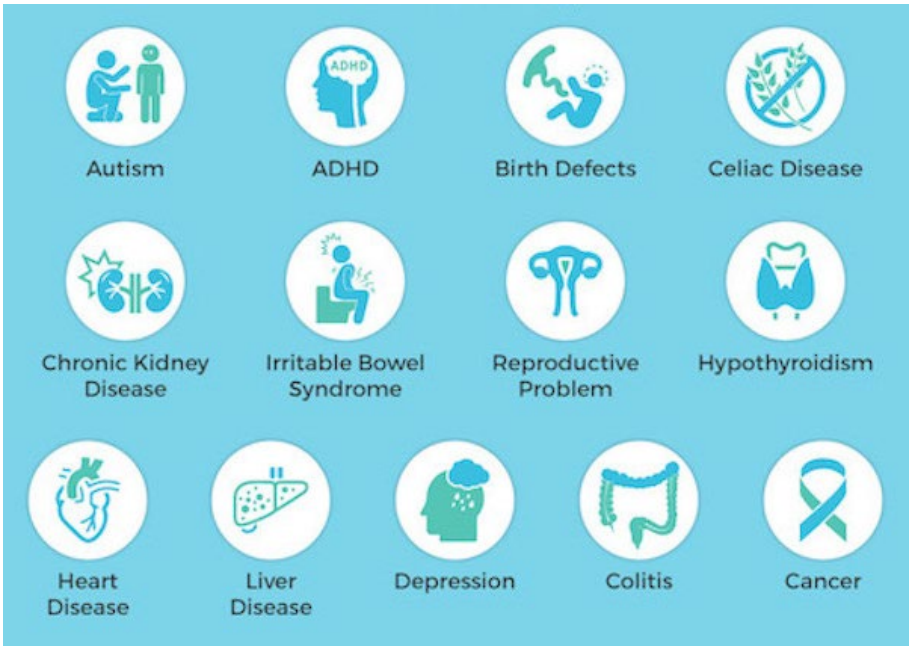

Figure 1.5: Various health effects associated with Glyphosate use[20].

There is wide acceptance to the fact that while concern regarding the risks of glyphosate exposure/intake is serious, more comprehensive studies are required to fully understand its impact and make an informed hypothesis.

1.4 Glyphosate- the Weed killer

Chemically, Glyphosate (N- Phosphonomethyl Glycine) is a derivative of glycine which the smallest amino acid that can be found in proteins. In the glyphosate molecule, one of the amino group hydrogen atoms is replaced by a phosphonomethyl group-this is represented in Figure 1.6

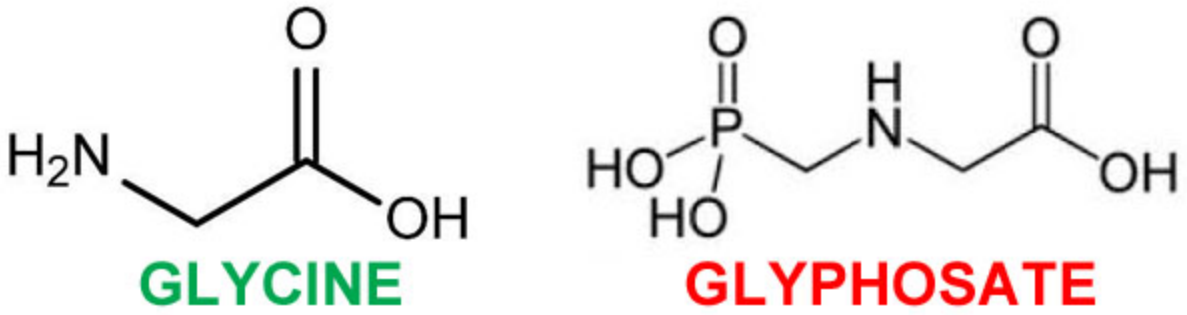

Figure 1.6: Comparing the chemical structures of Glyphosate and Glycine[41]

Glyphosate when absorbed by the plants binds to and blocks the enzymatic activity of the enzyme-enolpyruvylshikimate-3-phosphate synthase (EPSPS). This enzyme is part of the shikimic acid pathway that converts simple carbohydrate derived through glycolysis process and pentose phosphate pathway to aromatic amino acids and other plant nutrients or metabolites.

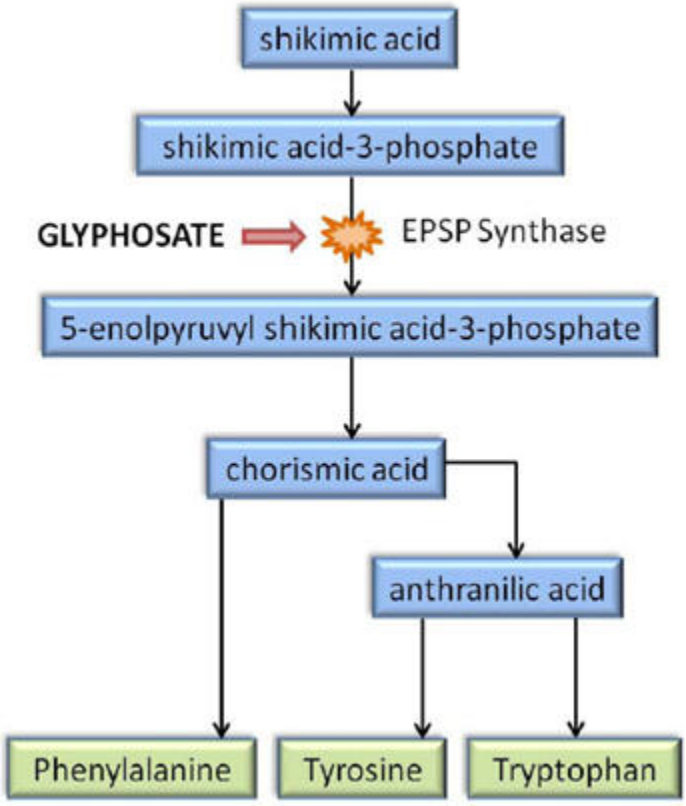

Figure 1.7: Pictorial representation of Glyphosate action inhibiting shikimic enzyme pathway[35]

EPSPS enzyme is normally present within the chloroplast in plants, where it catalyzes the shikimate-3-phosphate (S3P) and phosphoenol pyruvate reaction to form 5-enolpyruvyl-shikimate-3-phosphate (ESP). ESP acts as a precursor for aromatic amino acid production and thereby vitamins, hormones and other metabolites essential for the plant. Phosphoenol pyruvate structure is similar to that of glyphosate, hence this makes it possible for glyphosate to bind to the active site of EPSPS as we can see from Figure 1.7, inhibiting its activity.

The active site of the EPSPS enzyme is highly common in all higher plants, and hence glyphosate affects a broad spectrum of weeds indiscriminately as mentioned previously. Inhibiting the process of the shikimic acid pathway causes deficiency in aromatic amino acid production causing the plants to die due to lack of sufficient nutrients.[35]

CHAPTER 2

MOTIVATION

2.1 Current Detection methods

Various methods to analyze glyphosate have been developed and described in previous works. This includes techniques such as liquid chromatography-mass spectrometry (LC-MS), capillary electrolysis (CE) and enzyme-linked immunosorbent assays (ELISA). These are explained in detail in the following sub-sections.

2.1.1 Liquid Chromatography-Mass Spectrometry (LC-MS)

It is an analytical technique which combines the physical separation principle of liquid chromatography (LC) along with mass based analyzing capability of mass spectrometry (MS).

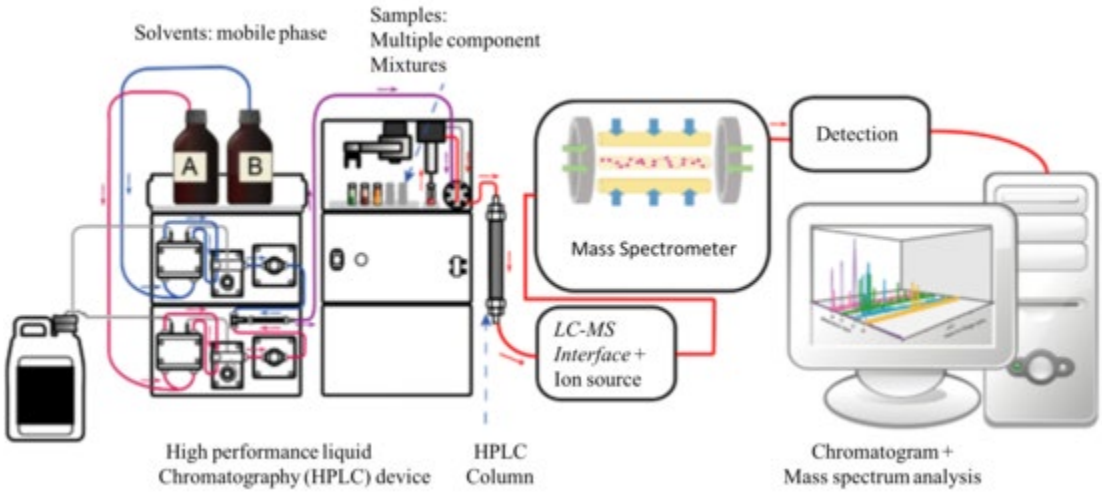

Figure 2.1: Graphical representation of an LC-MS integrated system[31]

Partition chromatography method [31] implemented makes use of non-polar, hydrophobic stationary phase and a polar mobile phase (liquid). Here, the test sample of interest (volume usually

around 20 μL) is injected into the mobile phase of the system. This conjugate containing the analyte is pumped under high pressure (upto 400 Bar/300,000 Torr) into the HPLC column (Figure 2.1) containing the stationary bed (phase) where the constituents of the conjugate mixture are separated depending on their chemical affinity with respect to the mobile and stationary phases. Separation occurs after repeated sorption and desorption steps which take place as the fluid sample interacts with the stationary bed. Depending on this separation between the two phases (mobile and stationary), the constituents of the sample will flow out of the column at different times.

Then, the sample is transferred to the MS system via the LC-MS interface integrated together with the ion source (Figure 2.1). This ion source transforms ions in sample from the liquid phase to gas phase while converting neutral sample molecules again into gas phase ions which are sent into the mass analyzer. Mass spectrometry technique measures mass-to-charge (m/z) of the ions by applying electric or magnetic field to separate ions by their masses which is captured by the detector system and analyzed to plot the Chromatogram along with mass spectrometry results. A representation of this kind of work was employed specifically towards the detection of glyphosate and is displayed in Figure 2.2.

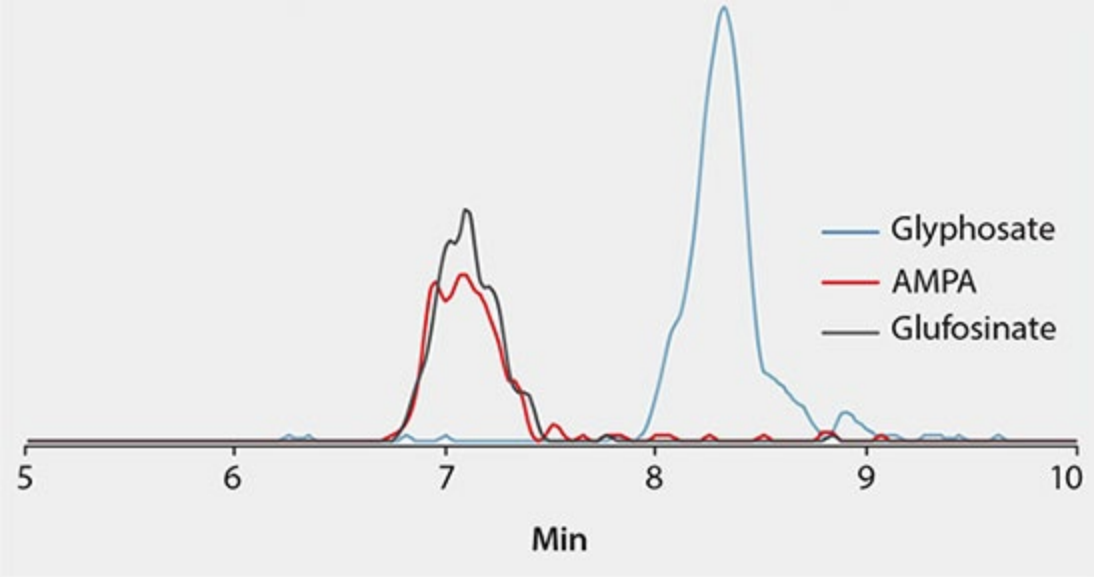

Figure 2.2: LC-MS analysis results for detecting Glyphosate in oats, wheat extracts.[22]

2.1.2 Capillary Electrophoresis (CE)

Capillary electrophoresis (CE) [32] has been used as a scheme for separating and detecting glyphosate coupled with indirect fluorescence or UV absorbance detection. It is an analytical method that separates ions based on electrophoretic mobility by applying a high voltage, the mobility is further dependent on a number of factors including charge of the molecule, viscosity of the medium, and the radius of the atom.

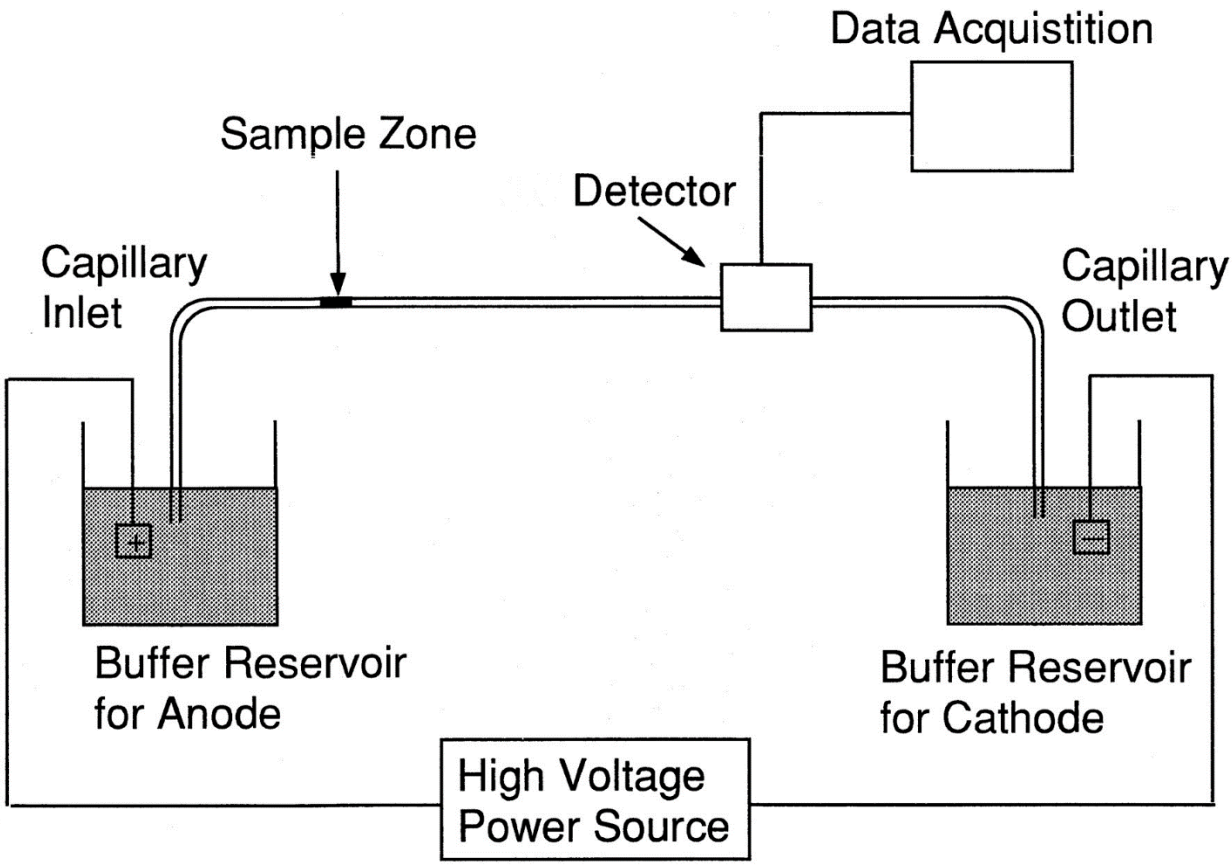

Figure 2.3: Functional Diagram depicting Capillary Electrophoresis (CE)[32]

From Figure 2.3, we deduce the typical setup of a CE system-a high powered voltage source is connected to two ends of an electrode (i.e. anode and cathode) dipped in a vial filled with buffer medium. The test sample is inserted into the anode vial usually through hydrostatic injection and activation potential is applied. The rate at which the constituent sample particle moves is directly proportional to this applied potential i.e. when the field applied is greater, the electrophoretic mobility increases.

Based on studies for detection of Glyphosate using CE, the capillary system is equilibrated with the running buffer under electric field around 250 V/m for a fixed period of time (approximately 30 minutes). The detector located near the cathodic end of the capillary (Figure

2.3) allows UV-VIS light to pass through the analyte and thereby able to measure the absorbance. Photomultiplier tube (Data Acquisition circuit) is also attached to this end enabling the construction of a mass spectrum graph, which gives useful information about the mass to charge ratio of the ionic species and is used to detect glyphosate in samples.

2.1.3 Enzyme-Linked Immunosorbent Assay (ELISA)

ELISA [28] is a micro-well plate based assay technique for detecting and quantifying various substances like peptides, antibodies and hormones. Antibody-Antigen interaction (i.e.) affinity based detection or sensing is the most crucial element of the principle. ELISA is used for rapid sample testing and accurate results while being known to be more cost effective than conventional chromatography methods.

To briefly explain the ELISA process [28], the surface of the micro-well plate is immobilized with the antibody. An enzyme is tagged with this antibody for colorimetric purpose. Next, Antigen is added to micro-well and this incubation for a preset period of time is followed by washing which removes the unbound antigen. The appropriate chromogenic substrate is added to the medium to produce a signal through a colorimetric response, the signal is then measured and a standard concentration curve is plotted to determine the amount of antigen in the sample. Displayed below in Figure 2.4 is the principle of ELISA described here along with pictorial representations of other types of ELISA techniques.

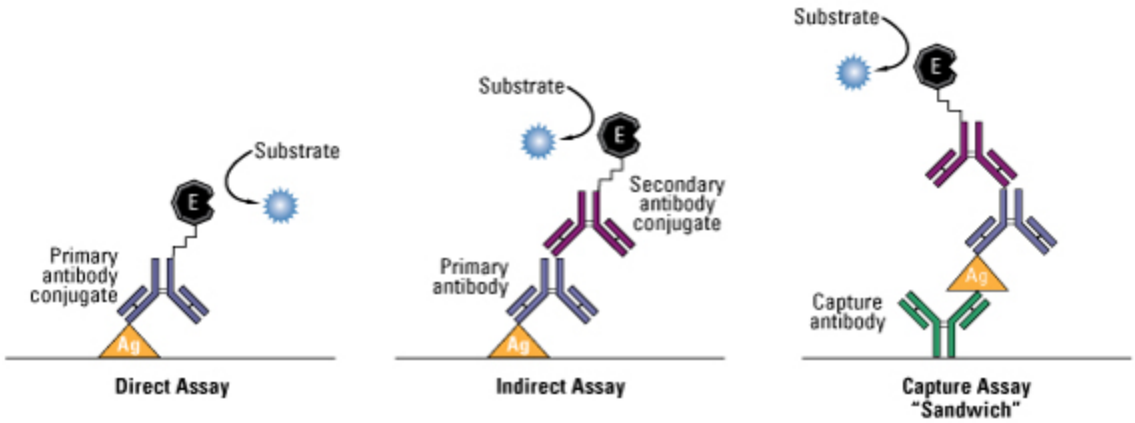

Figure 2.4: Diagram representing common ELISA technique types.[28]

For glyphosate detection [34], competition based ELISA has been used in commercially available kits. It is executed by designing the enzyme immunoassay in such a way that with only a limited number of antibody binding sites (Antibody bound to the micro-well plate in prior), glyphosate in test sample as well as glyphosate-Horseradish Peroxidase (HRP) conjugate are added together into the wells. When no glyphosate is present in the sample, the enzyme (HRP) tagged glyphosate will bind to the antibody binding sites resulting in high coloration while if a significant concentration of glyphosate is present in sample and binds to the antibody (active sites), then less of the enzyme (HRP) tagged glyphosate can bind to the antibody binding sites causing a decrease in coloration. Therefore, we conclude that the intensity of resultant color developed is inversely proportional to the concentration of glyphosate in sample.

2.2 Innovation:

Issues with the detection of glyphosate in field samples include the inability to report results in real-time accurately (i.e. without compromising sensitivity), high laboratory costs involved to perform comprehensive tests to determine contamination and also most importantly lack of a

quantitative sensing system that is portable. Hence, there is a need for such a field deployable test which addresses all of the above problems.

The innovation of this work lies in designing a Real-time, Portable Electrochemical Sensing system in the form factor of a handheld device. This system can detect trace levels of Glyphosate in produce samples while here, real-time implies that the system can give effective responses in under a minute. Low cost option as it is designed to target an everyday use audience that might not have lab training/experience with the overall value addition being that- An effective tool is developed that can be used consumers and industry alike to keep a check on food safety and quality.

Hence, an affinity based electrochemical sensing mechanism integrated with a custom electronics platform and machine learning model for analytics is established for real-time, portable detection of glyphosate pesticide.

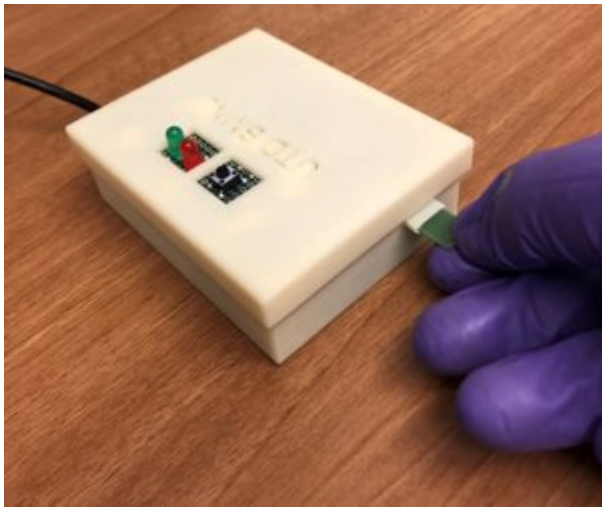

Figure 2.5: ELECTROCHEMSENSE prototype device designed at UTD-BMNL

CHAPTER 3

MATERIALS AND METHODS

3.1 Sensor Design

The Sensor chip was designed using a commercially available computer-aided design and drafting software-AutoCAD by Autodesk, this particular interdigitated electrode (IDE) design has been characterized for electrochemical sensing previously in our Lab (UTD-BMNL) and based of which design changes were added to the sensor design (Figure 3.3 and Figure 3.4) and dimensions to incorporate easy interfacing mechanism with the electronic reader device.

For this particular application, a 2-electrode system (Working Electrode [WE] and Reference Electrode [RE]) was preferred. As in the case of any 2-electrode system the Reference and Counter are shorted into a single electrode. Both the terminals of the electrode are designed such that it is symmetrical-therefore WE and RE can be used interchangeably.

3.1.1 Printed Circuit Board (PCB) Substrate

Sensor design described above is fabricated on a PCB substrate, manufactured in bulk by PCB Way (HK WEIKU Technology Company Limited, China). The fabrication was a single layer (Top layer) deposition with the conductive layer (copper layer), solder mask and overlay (silkscreen layer)-Here the conductive layer holds the immersion gold metal deposition and provides the electrical connectivity required for the sensor, while the solder mask provides insulation to the rest of the sensor region. The silkscreen layer is added for functionality and depicts sensor chip boundary regions thereby giving the necessary interfacing capability with the electronic reader (USB-Flash drive design to slot into reader port).

PCB substrate material type used in FR-4 TG-130 with thickness of 1.6mm (6/6 mil track/spacing), overall dimension of the sensor chip is 17.8 x 9.7 mm and Figure 3.1 represents the electrochemical sensor chip with the electrode region magnified and blown up for easier visibility.

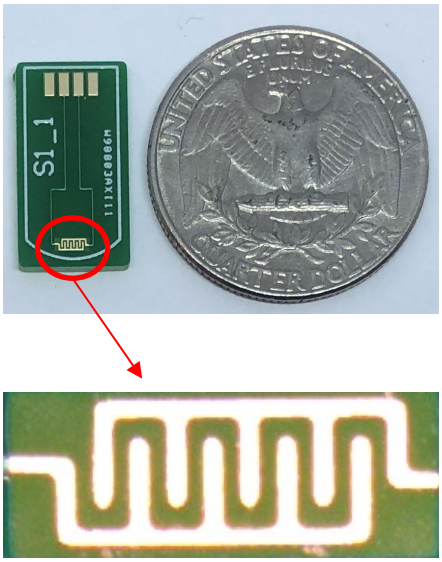

Figure 3.1: Sensor Image (2-electrode system) (TOP) and interdigitated electrode design (IDE) (BOTTOM)

3.1.2 Electrode Dimension

Electrode geometry plays a vital role in determining the effective signal threshold due to the chemical interactions and directly impacts the sensitivity to detect small changes in the overall signal. In addition to the geometry itself, electrode size/dimension is important towards the signal response and thereby, sensor performance.

Interdigitated Electrode (IDE) Figure 3.2 is the electrode geometry adapted for this sensing system, where the width of the gold region is 0.15 mm and the dimensions are 2 x 0.675 mm. Electrodes are shaped with rounded edges to prevent accumulation of charges around the corners/edges.

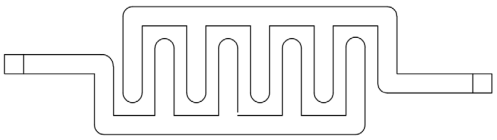

Figure 3.2: Interdigitated Electrode Geometry used in this application

The following sensor designs (same Electrode geometry and specification) were considered:

Design 1:

To increase the functionality of the sensor design, the sensor chip (Figure 3.2) was designed by replicating a micro SD card design.

The feasibility of this design is considered with respect to the following factors:

1. Ease of fabrication
2. Connector design to interface with electronic reader
3. Programming constraints

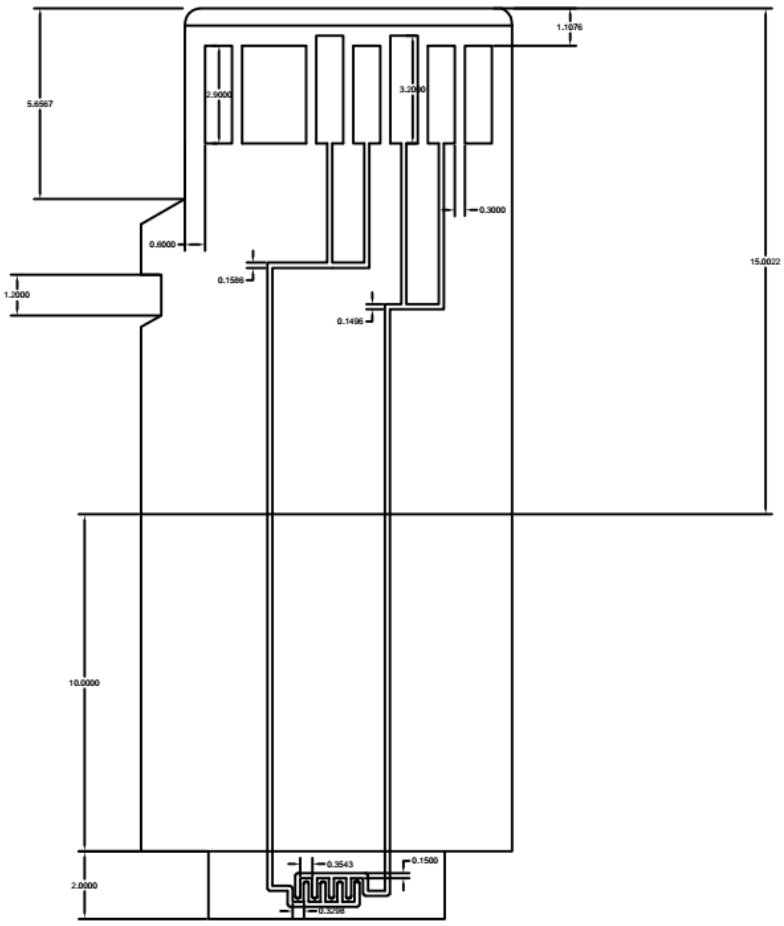

Figure 3.3: Sensor Design 1 (Micro SD card replicate structure)

Design 2:

Similar to the previous design, the intent of increasing functionality and also keeping in mind fabrication, interfacing and programming constraints- a sensor chip replicating a USB Flash Drive is drawn using the CAD software.

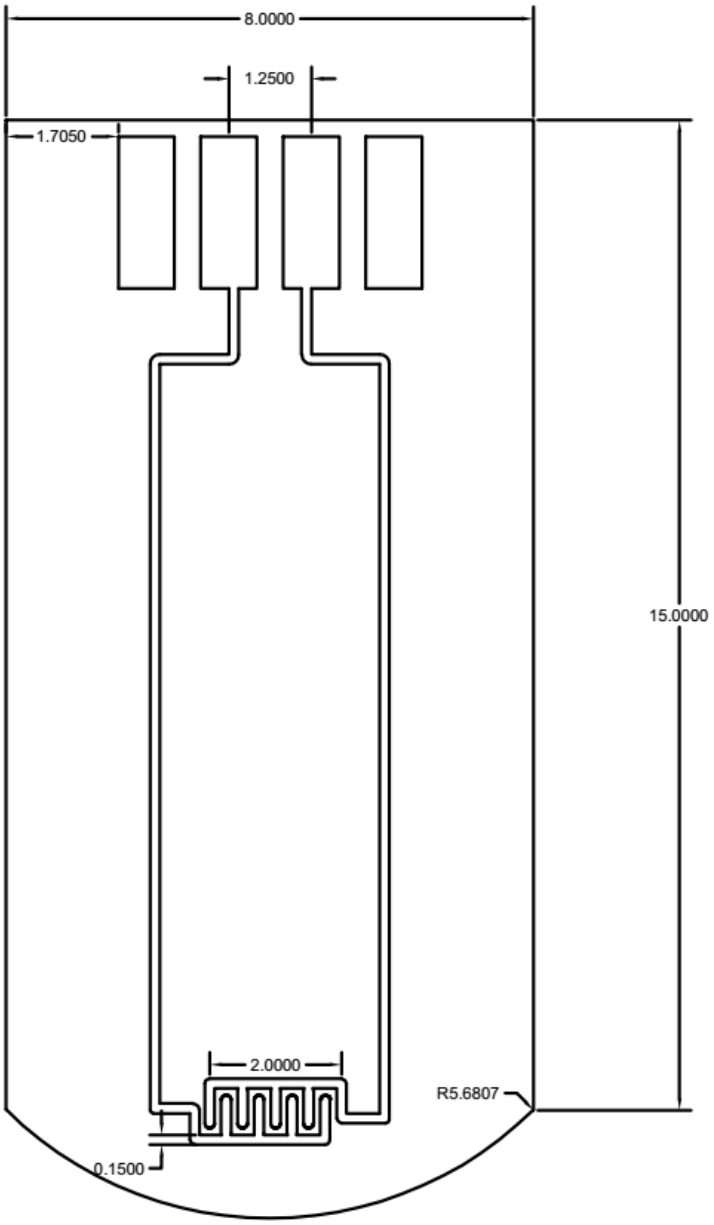

Figure 3.4: Sensor design 2 (USB Flash drive structure)

3.1.3 Sensor Characterization

3.1.3 A) Electrode Geometry Characterization to determine Feasibility:

Interdigitated Electrode (IDE) design from Figure 3.2 is characterized using Finite Element Analysis (FEA) with the help of COMSOL Multiphysics software. Modelling parameters are given

in Table 1, and along with the activation conditions-they are used to simulate the actual sensor performance.

Table 3.1: Modelling Parameters used in COMSOL simulation

Parameter	Value
Electrical Conductivity: Gold	$4.13 * 10^{7}$ S/m
Electrical Resistivity: Gold	$2.83 * 10^{-5}$ Ω.m
Temperature Co-efficient: Gold	0.0034 K^{-1}
Dielectric Permittivity (ε): Gold	6.9
Electrical Conductivity: PBS	$1.8 * 10^{-3}$ S/m

Table 3.2: Activating Condition (Potential Stimulation of Electrode Terminal)

WE	Φ=500 mV
RE	Φ=0 mV

Modelling parameters are given in Table 1, and along with the activation conditions in Table 2-they are used to simulate and capture the actual sensor performance/response.

3.1.3 B) Contact Angle and Optimal Volume Study:

Contact angle measurements are captured with a Ramé-Hart goniometer tool to determine the surface properties of the rigid PCB substrate and analyzed using the DROPimage software. Next, the optimum fluid volume is determined by performing a drop test using a standard buffer solution (PBS) with and without red food coloring for better visibility.

3.2 Buffers, Reagents and Chemicals

3.2.1 Dithiobis (succinimidyl propionate) [DSP] - Lomant's Reagent

Dithiobis (succinimidyl propionate) [40] contains an amine-reactive N-hydroxysuccinimide (NHS) ester on either end along with a cleavable disulfide bond in its spacer arm as can be seen from Figure 3.5. The disulfide bond is cleaved in the presence of gold wherein it forms a thiol-linkage

with the electrode surface and holds two NHS-ester amine reactive groups on the other end. NHS-esters react with primary amines to form stable bonds. Proteins, including antibodies, generally have several primary amines in their side chains and this principle is exploited to immobilize antibodies to the gold surface via the cross-linker.

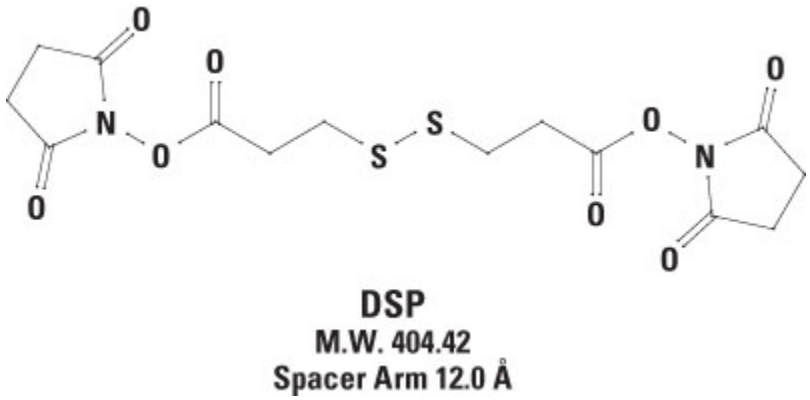

Figure 3.5: Chemical Structure of Dithiobis (succinimidyl propionate) cross-linker[40]

DSP (Thermo Scientific, USA) is a widely used cross-linker in protein binding applications, its chemical properties are summarized in Table 3. In our application, we have used DSP to serve as the linker between the gold surface on the electrode and the antibody.

Table 3.3: Summary of Dithiobis (succinimidyl propionate) [DSP] Properties[40]

Alternative names	Lomant's reagent, DTSP
Molecular formula	$C_{14}H_{16}N_2O_8S_2$
Molecular weight	404.42
Spacer arm length	12.0 Å (8 atoms)
CAS number	57757-57-0
Storage conditions	4°C, protect from moisture, use only fresh solutions
Reactive groups	NHS esters, react with primary amines at pH 7.0-9.0

3.2.2 Phosphate Buffer Saline (PBS)

Dulbecco's phosphate buffered saline (Thermo Scientific, USA) is a balanced salt solution and was used to prepare and reconstitute the antibody and target pesticide (Glyphosate) as well as the produce extract solutions. PBS is an isotonic and non-toxic buffer maintained at pH 4.3-4.7. The concentration used for serial dilutions and other applications was 10 mM (10X PBS). The buffer contents include calcium and magnesium inorganic salts. PBS is highly popular and used for spectrum of applications from mammalian cell culture applications, to increase the longevity of stock proteins when used over a course of time.

3.2.3 Produce Run-Off/Extract solutions

For this study, experiments were conducted on run-off/extract solutions obtained from Apples, Strawberries, Bell Peppers and Carrots. To start off, pulp was extracted from sliced pieces of apple samples utilizing pestle and mortar to mash them gently-this pulp extract from each produce served as 1 part to which 4 equivalent parts of 10X PBS was added and mixed (vortexed) before centrifuging it at 13,000 rpm for 2 minutes to produce the required produce extract solution. This same process is then repeated for strawberries and bell peppers. For Carrots, we adopt another

procedure to obtain run-off solution by washing small pieces of carrot with 1 mL of 10X PBS before centrifuging at 13,000 rpm for 2 minutes. By this method produce run-off/extract solutions are obtained for all of the samples.

3.2.4 Glyphosate Antibody and Antigen

Glyphosate comes under the family of organophosphorus pesticides/herbicides, with its structure as represented in Figure 3.6. It is a derivative of phosphonic acid and glycine [50]. It was obtained in powder form from Sigma Aldrich, USA and reconstituted in PBS to 1mg/mL concentration, then it was mixed using pipette action and stored at 4°C for short term use. This is the stock solution of glyphosate antigen and was further serially diluted as needed for experiments.

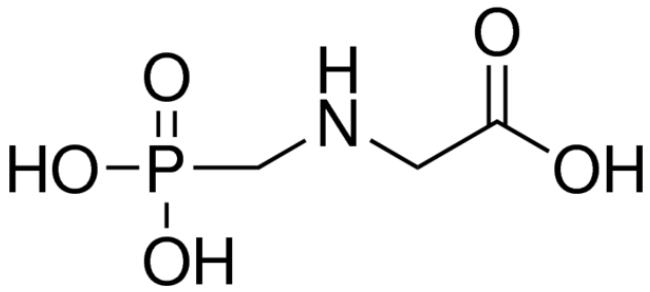

Figure 3.6: Chemical structure of Glyphosate (N-(Phosphonomethyl) glycine)[42]

Antibodies are produced by the immune system when any foreign body or immunogen enters the system [43]. Here, we use Polyclonal Glyphosate antibody (Fitzgerald Antibodies, USA) of IgY isotype extracted from a chicken host where a BSA-Glyphosate conjugate was used as the immunogen and injected into the host. The antibody was obtained at 5mg/mL stock concentration and was reconstituted according to experimental requirement. Small aliquots of diluted antibody solution was stored short term at 4°C and the stock was maintained long term at -20°C.

In a Brief explanation [43] [4], antibodies are immunoglobulins i.e. immune system related proteins which consists of 4 polypeptide chains out of which 2 are heavy chains and 2 are light chains as depicted in Figure 3.7. These 4 polypeptide chains are joined together to form the Y-shaped molecule structure of the antibody.

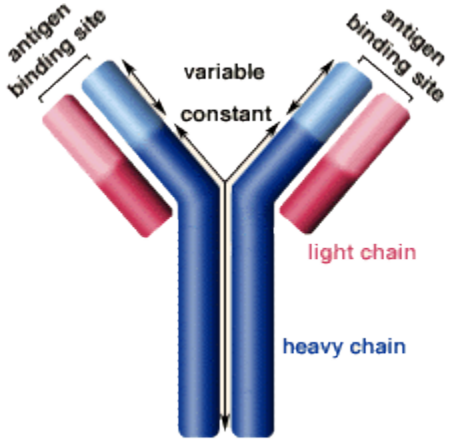

Figure 3.7: Structural Anatomy of Antibody molecule[43]

The primary amine group in the heavy chain of the Y-shaped molecule chemically interacts with NHS-ester ends of the DSP cross-linker immobilized onto the gold surface to form stable amide bonds. Further, the 'arm-tip' region of the Y-shaped antibody molecule is depicted as the variable region as the amino acid sequence varies in this area. This is the region composed of 110-130 amino acids and gives specificity towards the binding antigen, and hence acts as the binding site for the antigen to interact with antibody.

3.3 Immunoassay Protocol

The experimental protocol to construct and characterize sensor immunoassay stack depicted in Figure 3.8 is given as follows. Sensing modality used to characterize the response in all of the experiments is Chronoamperometry (CA). Sensor preparation involves soldering copper wires to the gold connector leads of the sensor and subsequently cleaning the surface with IPA and DI water before using the Nitrogen gas spray-gun to dry the surface. The whole protocol is devised for one individual chip and each chip is dosed serially from the lowest to highest dose (Ascending order).

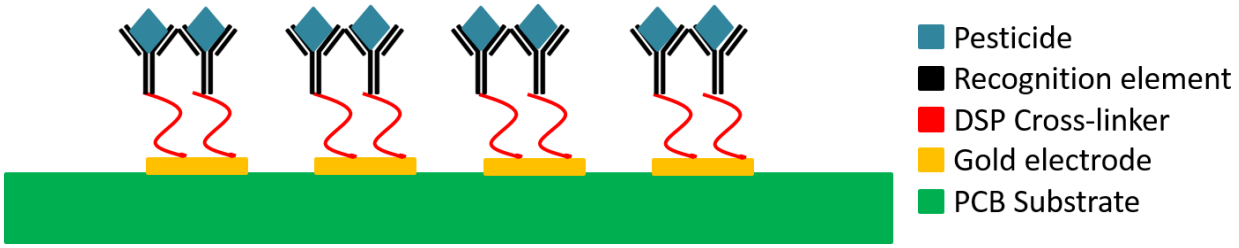

Figure 3.8: Electrochemical sensor Immunoassay stack

Once the sensor is prepared, 5 µL of DSP made in dimethyl sulfoxide (DMSO) is dispensed onto the gold electrode sensing region and incubated for 1.5 hours-thereby, giving enough time for the DSP molecules to get immobilized to the gold surface. Also, the sensor is incubated in a humidifying chamber (must be dark since DSP is light sensitive) to ensure that DSP or any dispensed fluid does not evaporate. At the end of the incubation time, take CA measurement by applying 500mV step signal for 30 seconds and a negative step of -500mV for another 30 seconds and record the result. After this step is completed, the sensor surface is aspirated completely and 5 µL of blank DMSO is dispensed to the sensor surface to wash off the unconjugated DSP. The sensor surface is again aspirated completely and dried with nitrogen before adding 5 µL of

Glyphosate Antibody solution of 500 µg/mL (serially diluted from stock concentration of 5 mg/mL) concentration and allowed to incubate undisturbed for 30 minutes. Similar to the DSP step, once the incubation time is complete-CA measurements are taken with the same conditions as mentioned previously. Wash the sensor surface using 5 µL of PBS to remove unbound antibody and then aspirate completely till dry. Next, 5 µL of superblock (Blocking buffer) (Thermo Scientific, USA) is dispensed to the electrode surface and incubate for 10 minutes-this step is performed to minimize unspecific binding by using a blocking buffer medium. CA measurements are taken at the end of 10 minutes as per the original conditions. Remove the fluid and aspirate till electrode surface is dry.

The glyphosate antigen doses are serially diluted using PBS from stock concentration of 1 mg/mL to a range of concentrations required between 10 ng/mL – 50 µg/mL. Blank PBS (Baseline/Negative control) is added to the sensor surface and incubated for 5 minutes. CA measurements are taken similar to the original setting. Then, the fluid is aspirated from the electrode surface and this procedure is repeated for the all doses in ascending order for the same interval of 5 minutes to promote antigen-antibody binding to take place.

After completing the above steps for all the doses prepared in PBS (Synthetic Glyphosate Sample), the doses are prepared serially again in produce run-off/extract solution instead of PBS in a similar manner. Once the doses are prepared, the same steps as above is repeated to take CA measurements for each dose in produce solution (Here, unspiked produce run-off/extract solution acts as negative control).

Each of the above experiments are repeated for N=5 replicates to prove repeatability.

3.4 Validation of immunochemistry using FTIR [2] [3] [6]

Gold electrode surface modifications by conjugation of DSP linker molecules followed by antibody was validated using FTIR analysis. Functionalization of electrode surface was carried out as described in the previous section. Prior to FTIR measurements, the sample was thoroughly washed with DI water and subsequently dried with N2 air to get rid of any unbound material that may interfere with the analysis. The infrared spectra of surface functionalized samples were recorded with a Nicolet iS50 FTIR spectrometer. Absorbance spectral measurements were obtained with a scan resolution of 4 cm−1 for 64 scans in the spectral range of 4000 cm−1 to 600 cm−1. Absorption spectra was recorded first for the Glass-Gold surface conjugated with only DSP molecules, and then Glass-Gold surface with antibodies linked via the DSP cross-linker.

CHAPTER 4

RESULTS AND DISCUSSION

4.1 Electrode Characterization using COMSOL Multiphysics simulation

Finite element analysis (FEA) performed on the Interdigitated Electrode (IDE) design geometry based on the activating conditions mentioned in the previous section [10]. The Electrolyte Potential and Current density was analyzed using secondary current distribution module in COMSOL Multiphysics.

In Figure 4.1, the plot with electrolyte potential (Bottom) depicts the surface potential at the WE (where the activation potential is applied) against the RE (which is maintained at ground). Current density investigates the variation in charge distribution which is visualized in the Figure (Top-Right) with a line plot as we move from WE-RE (Boundary conditions depicted in Figure 4.1 Top-Left).

Secondary Current Distribution [51] accounts for losses due to solution resistance as well as effects related to electrode kinetics. Concentration dependent effects are not considered in this model. This particular model is used to estimate activation losses and showcase proof of design feasibility for this application before taking into account concentration dependent reaction kinetics. The assumptions about the electrolyte composition and properties are the same as for the primary current distribution model, resulting in Ohm's law for electrolyte current. However, Secondary Current distribution model makes the following assumptions: convection within the electrolyte does not significantly affect current density, the electrolyte is homogeneous, but the potential of the electrolyte–electrode interface may be different from its equilibrium value.

Based on these assumptions, the following equations govern within the system:

$$J_{electrode} = -\sigma_s . \nabla . \phi_s \text{ with } \nabla . J_s = Q_s$$

….Equation 1

$$J_{electrolyte} = -\sigma_l . \nabla . \phi_l \text{ with } \nabla . J_l = Q_l$$

….Equation 2

$$\eta_m = \phi_s - \phi_l - E_{eq,m}$$

….Equation 3

In the above equations, J represents the current density (A/m2), and σ represents conductivity (S/m), while φ signifies electric potential (V). In the equations, the subscript‘s’ depicts the electrode domain, while the ‘l’ subscript denotes the electrolyte domain. $E_{eq,m}$ represents the potential difference at the electrode–electrolyte interface at equilibrium.

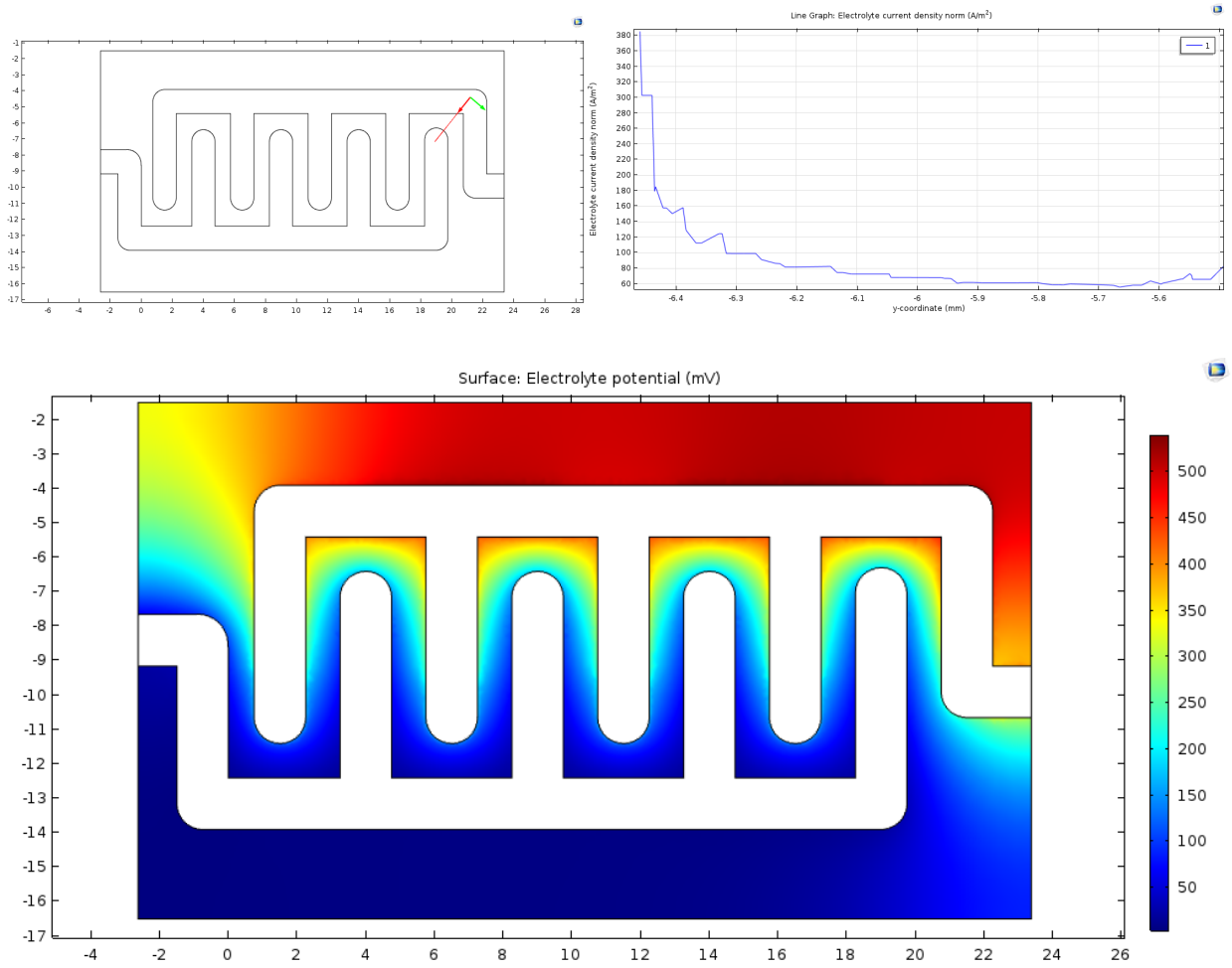

Figure 4.1: Line plot (Top-Right) demonstrating the current density distribution along the red line (Top-Left) which depicts WE-RE variation and Contour plot depicting surface electrolyte potential distribution (Bottom)

Therefore, from the results of the COMSOL simulation we infer that Current density is maximum around the working electrode and decays towards zero as it approaches RE. Also, Potential distribution is maximum around WE as we would expect.

4.2 Contact Angle and Optimal Volume Study

Contact angle measurements were taken using the Goniometer instrument and for the rigid PCB substrate coated with immersion gold, the contact angle of 60° (average value ≃ 62°) suggests a hydrophilic interface and hence can be used for this biosensing application. The solid-liquid interface captured is shown in Figure 4.2 below.

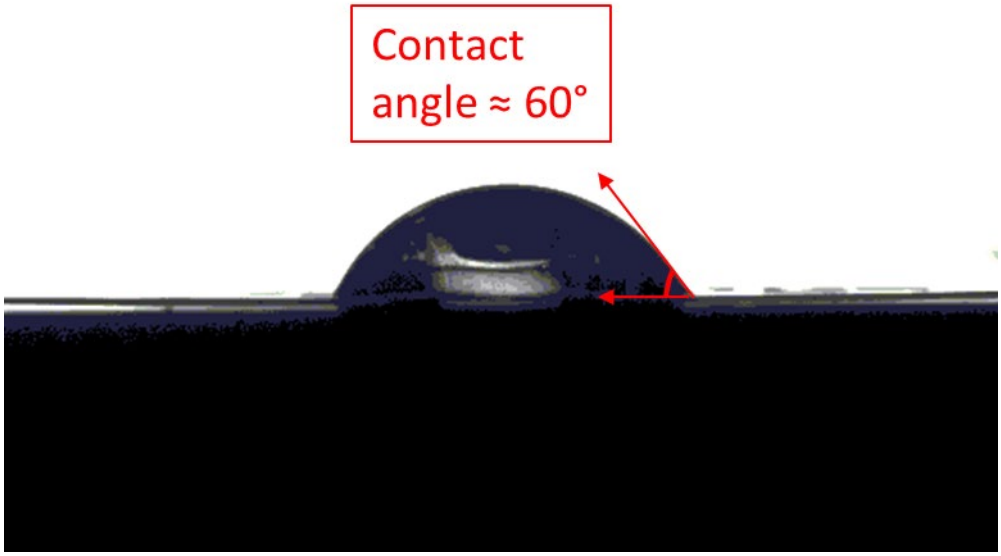

Figure 4.2: Solid-Liquid Interface to determine Contact angle made by fluid on PCB substrate

Further, to determine optimal volume required by the electrode surface for this application- the drop test with 5 µL volume yielded satisfactory results which can be visualized in Figure 4.3. For better visibility, (from, Figure 4.3) (A) Electrode region dispensed with buffer solvent (B) Electrode region dispensed with buffer solvent in red food color mix to highlight that electrode region is fully encompassed by the buffer solution.

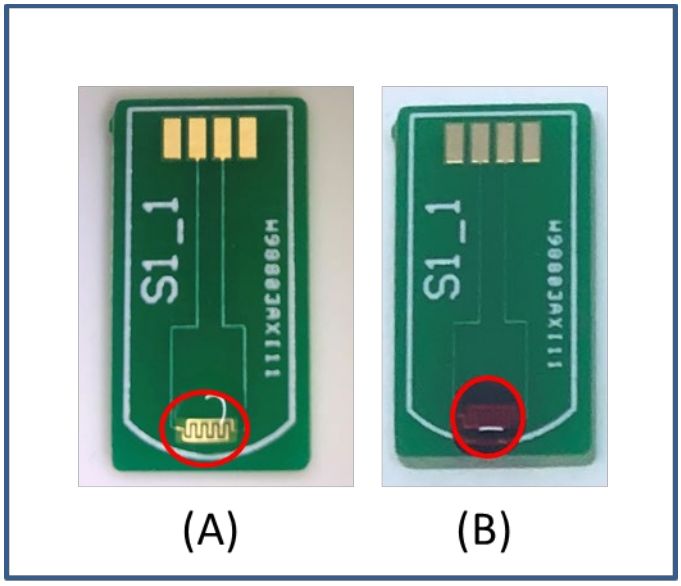

Figure 4.3: Drop test with (A) PBS solution (B) PBS solution in red food coloring to determine optimal fluid volume

Hence, Contact angle and Drop test results clearly display that 5µL is the optimum volume and that the PCB substrate can be utilized for this application.

4.3 Validation of immunochemistry using Fourier-transform infrared spectroscopy (FTIR) [2] [3] [6]

To confirm the chemisorption of DSP onto the gold surface we first analyzed the absorbance peak observed in the DSP spectrum, depicted in red in Figure 4.4 at 1741 cm^{-1} which is attributed to the symmetric carbonyl stretch of the NHS-ester. Furthermore, the peaks at 1450 cm^{-1} and 1370 cm^{-1} indicates the CH_2 and CH_3 group bending in DSP molecule. The reaction between the NHS-ester group and the primary amine group in the antibody molecule can be noted in the DSP + Antibody (AB) spectrum depicted in the Figure as the blue absorbance curve. C–O bonds of the NHS ester break down and react with the antibody amine group, resulting in a stable amide bond. Suppression

of peak characteristic of NHS ester (1741 cm^{-1}) is observed, whereas new peaks formed at 1540 cm^{-1} and 1650 cm^{-1} are characteristic of amide-I and amide-II peaks.

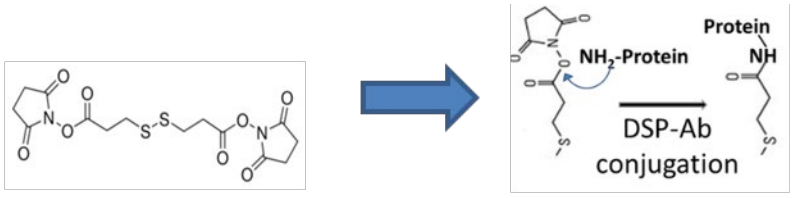

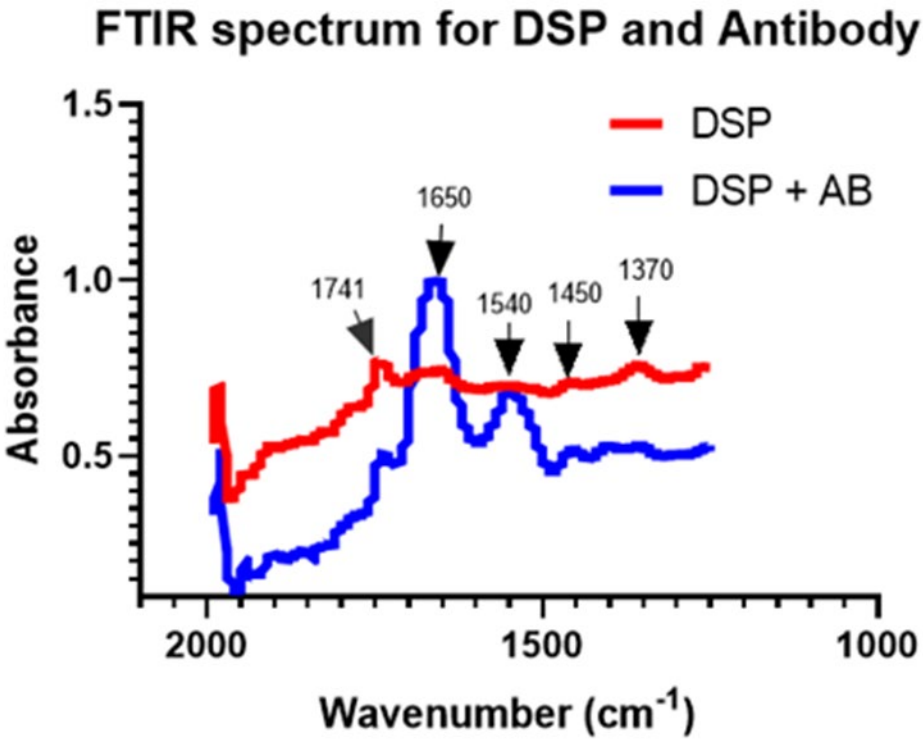

Figure 4.4: FTIR Spectrum of DSP (Red) and DSP-AB (Blue) to validate immunoassay chemistry

The results summarized in Table 4 signifies stable formation of immunoassay stack through the binding of the Glyphosate Antibody to the DSP-functionalized surface and validates the chemistry.

Table 4.1: Summary of FTIR absorbance peaks with their characteristic trait

Peak position	Implication
1741 cm^{-1}	Symmetric carbonyl stretch of NHS in DSP linker
1450 cm^{-1}	CH_2 bending
1370 cm^{-1}	CH_3 bending
1540 cm^{-1}	Amide-I Bond
1650 cm^{-1}	Amide-II Bond

4.4 Antibody Saturation Study

To determine the optimum antibody parameters for the experimental protocol and determine suitable concentration, an antibody saturation study was conducted. Anti-Glyphosate polyclonal antibody was obtained at 5 mg/mL concentration and diluted serially to a range of concentrations between 10 µg/mL to 1 mg/mL. Post DSP incubation and wash steps on N=3 sensor chips as given in the immunoassay protocol from the previous chapter, Antibody of lowest dose was dispensed onto the chip and incubated for 30 minutes after which CA measurement was taken and recorded. This process was further repeated in ascending order for the other remaining doses.

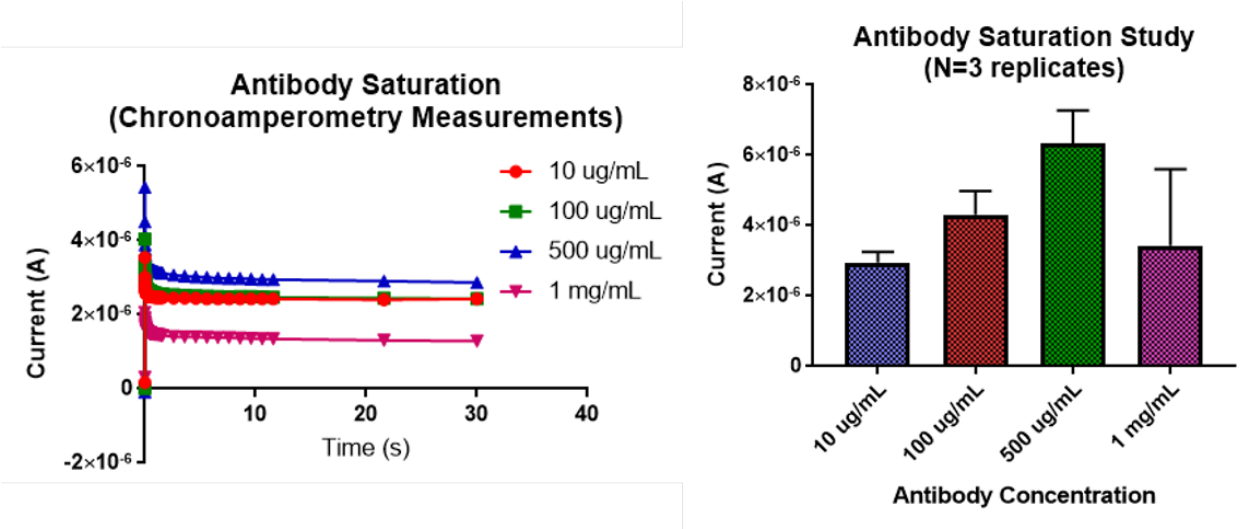

Figure 4.5: Antibody Saturation Study-Results

The results from the test is given in Figure 4.5, where it is clearly noticeable that the current values increase in a linear manner as we increase the dose concentration in the range between 10 µg/mL to 500 µg/mL after which at dose point- 1 mg/mL, the sensor saturates and current value drops rapidly. Hence 500 µg/mL was determined to be the optimum antibody concentration for the ElectrochemSENSE system.

4.5 Study of Electrochemical Sensor Response in various Samples tested on Potentiostat Lab Instrument

In this section, the electrochemical response of the sensor to detect glyphosate in multiple samples is tested using the Laboratory Potentiostat Instrument-Gamry. Since, the calibration as well as resolution of this system is well characterized over its use in the scientific community for many years-it was considered for the sake of this study as the standard to measure the ElectrochemSENSE system against.

When implementing the experimental protocol (N=5) on a synthetic sample (Antigen dose prepared with PBS buffer), the increase in current response is observed when sensor is serially dosed at concentrations between 0.01-10ppm (as displayed in Figure 4.6). Calibrated dose response (CDR) is determined by plotting the current fraction against concentration.

$$\textbf{Current Fraction} = (\textbf{Current}_{\textbf{dose}} - \textbf{Baseline Current}) / \textbf{Current}_{\textbf{dose}}$$

….Equation 4

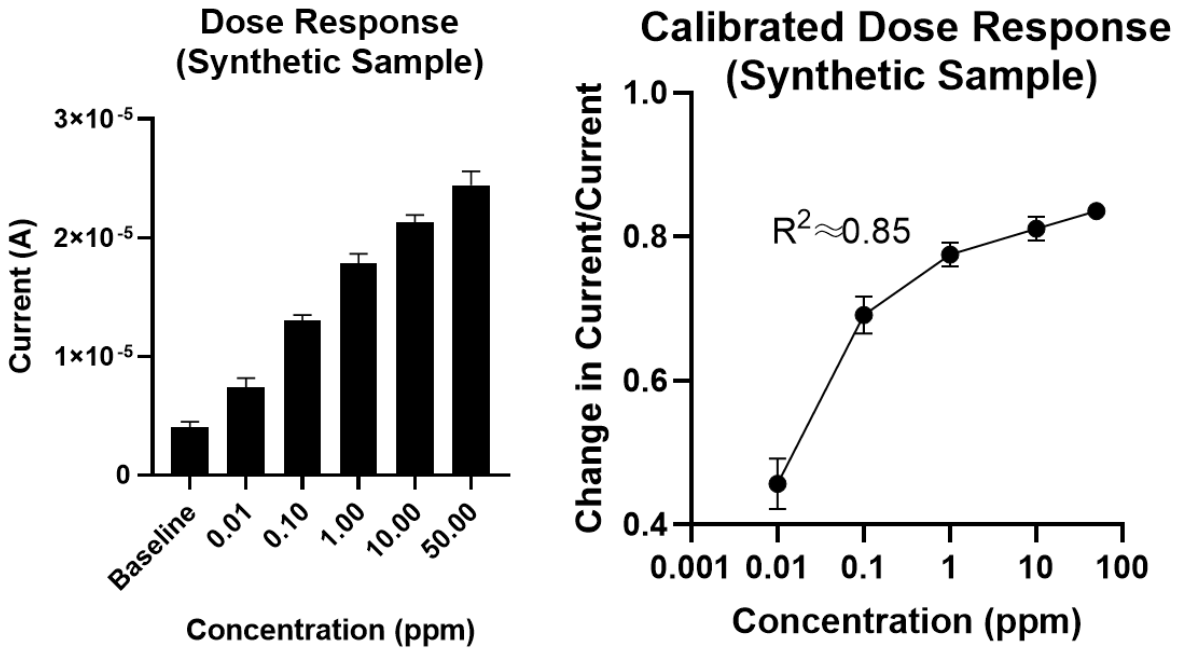

Figure 4.6: Dose response for Synthetic sample (left) and calibrated dose response curve (right)

It was noticed that, at and above 10 ppm the system seems to approach saturation level (i.e. current change is decreasing to a negligible level in CDR curve). Hence, another metric was determined based on MRL database table and CDR extraction to analyze each produce sample called Field Operating Range (FOR). It was inferred that the highest MRL in this study does not

exceed 5 ppm while the lowest is 0.1 ppm and hence the region of interest lies between 0.1 ppm and 5 ppm where maximum signal threshold is captured.

Next, experiments were repeated for each produce sample wherein the sensor (N=5) was dosed at low, MRL and high concentrations based on values from the MRL table for the particular produce group. The dose response for this set of experiments is represented in Figure 4.7. Similar to the CDR extraction of synthetic sample by using equation 4, the CDR plots for all produce samples are given in Figure 4.8. when sensor is serially dosed with glyphosate spiked produce samples at low, MRL and high concentrations, steady linear increase in signal with concentration is observed with R^2=0.99 (averaged for all produce).

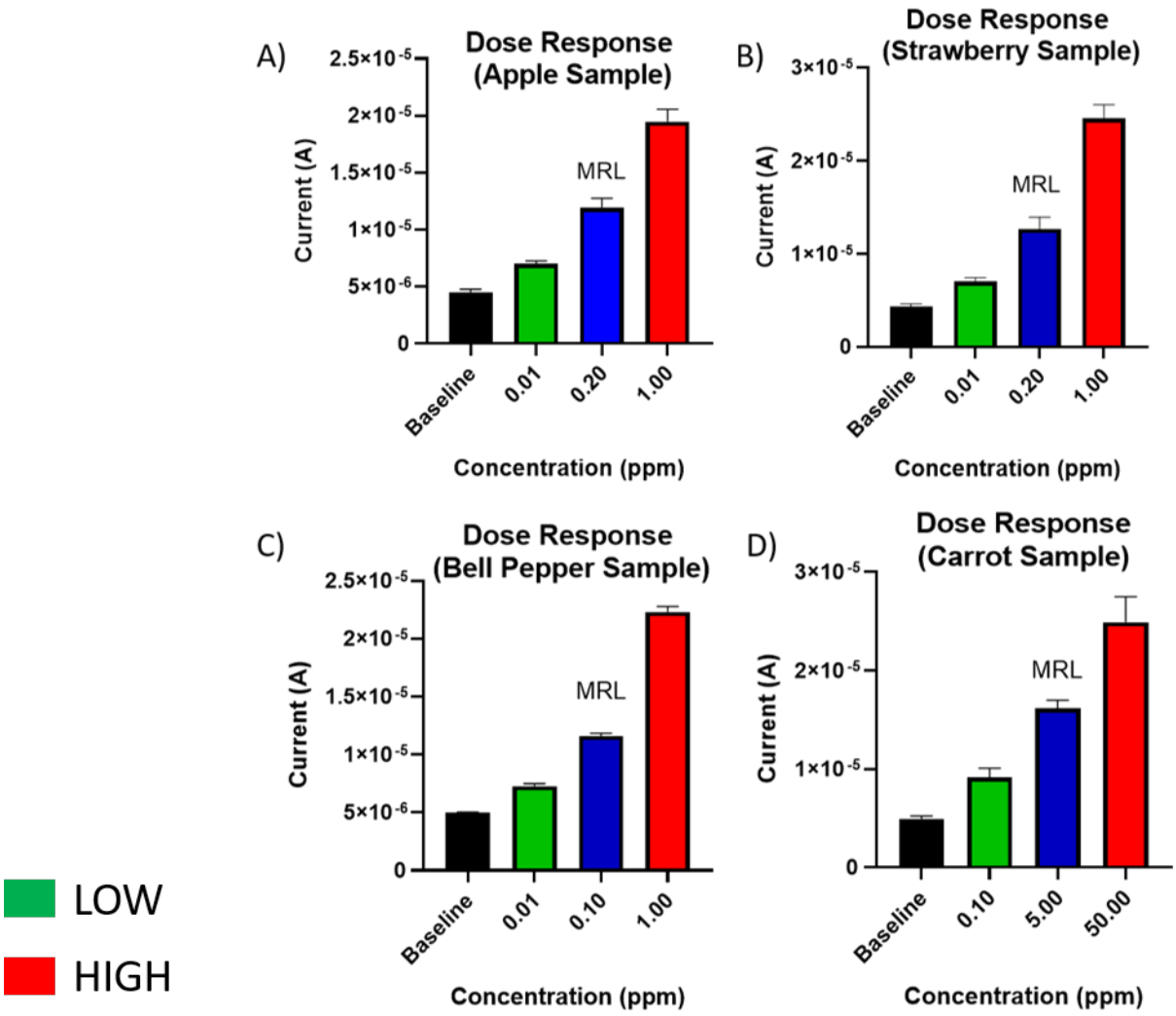

Figure 4.7: Dose Response for produce sample (A) Apple (B) Strawberry (C) Bell Pepper (D) Carrot determined using Lab Potentiostat Instrument

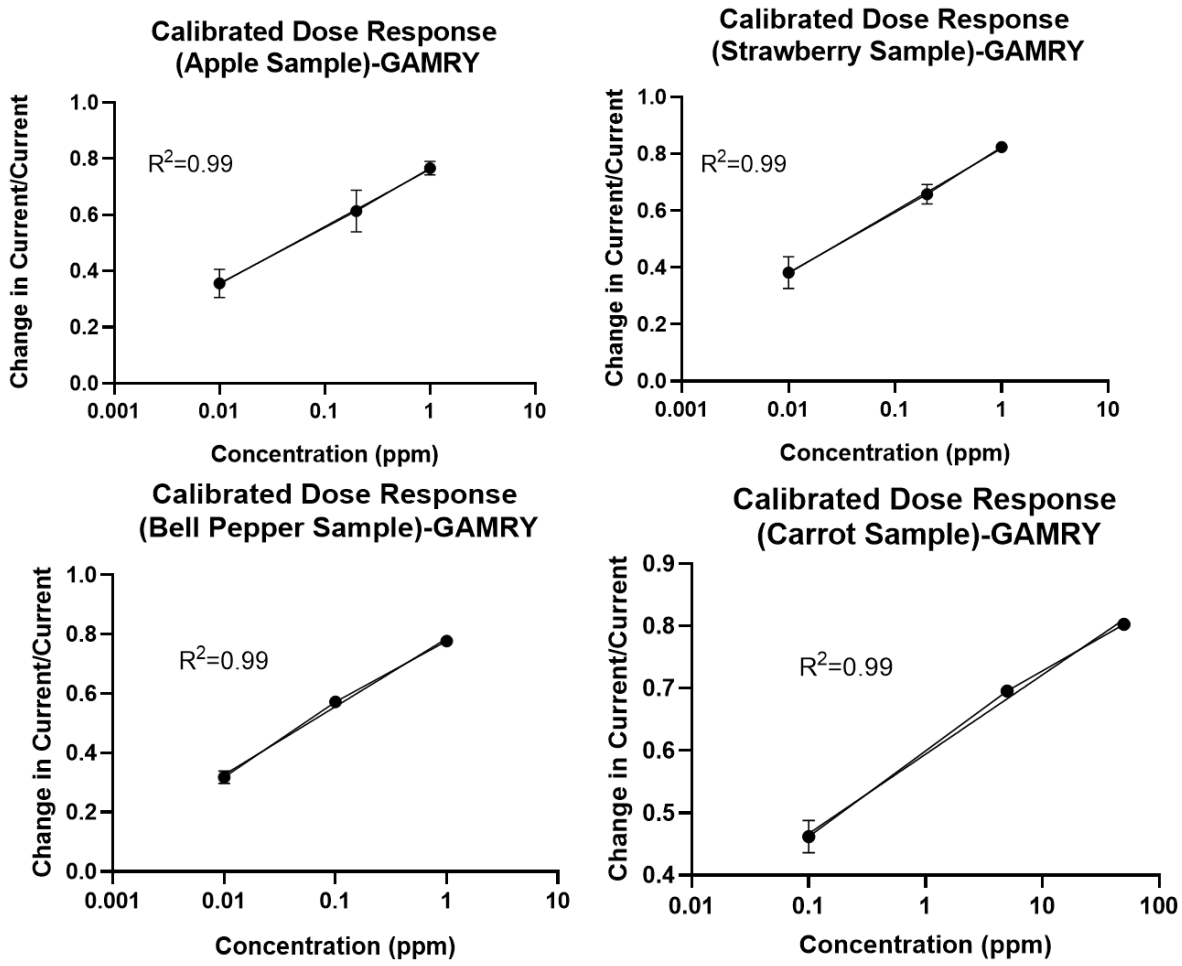

Figure 4.8: Calibrated Dose Response graphs for all produce samples

Next, to study if the CDR from the designed electrochemical sensor is able to detect random test doses-Another study was performed and the results were plotted. The Calibrated vs Test Response plot as shown in Figure 4.9 depicts that random test doses could be detected within the respective SAFE/UNSAFE range correctly based on the MRL value for each produce group although some deviation from CDR was observed. To quantify this deviation, Concentration recovery was used as the metrics and the data was tabulated (given in Tables 5-8). Here,

concentration recovery was obtained by plotting the observed current value into the CDR line equation ($y=mx+c$) for each produce.

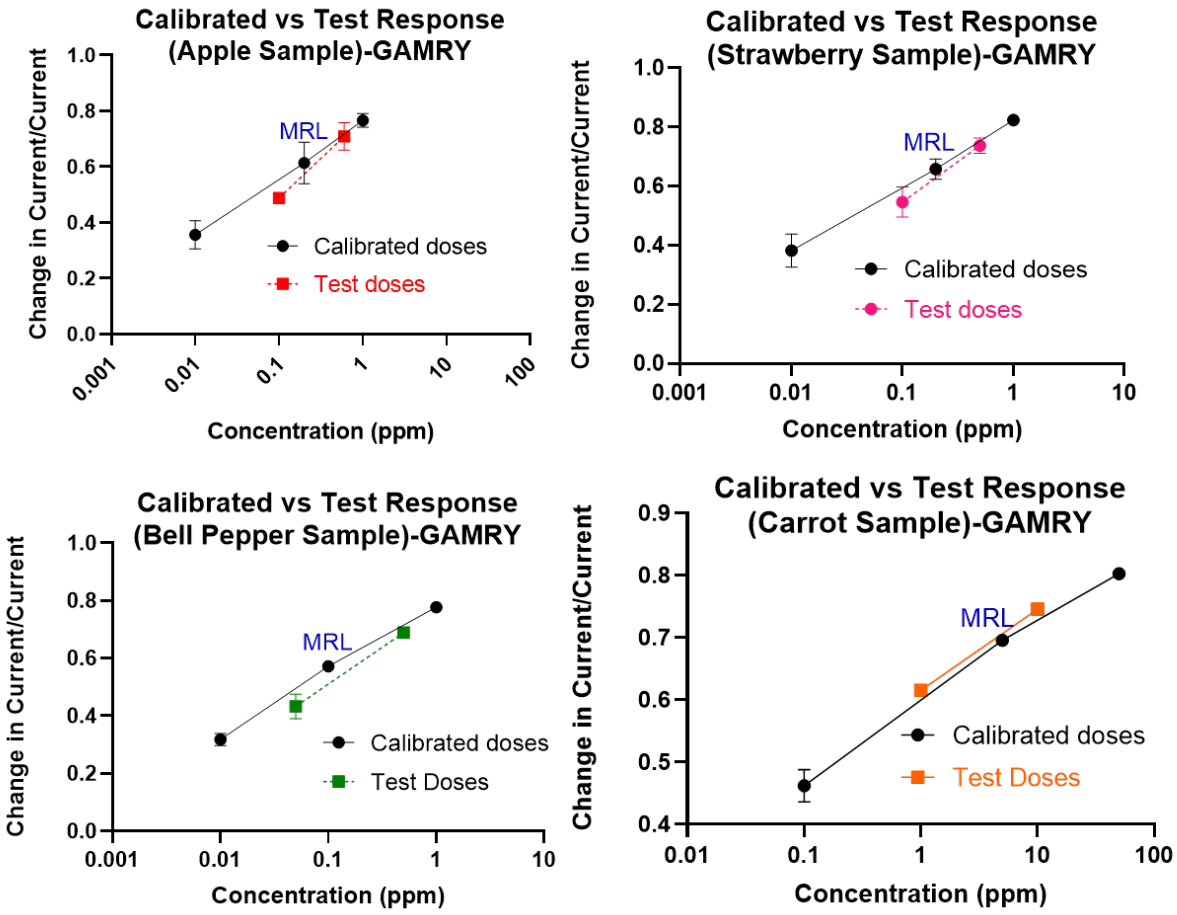

Figure 4.9: Calibrated vs Test Response for all produce samples (consolidated)

Table 4.2: Concentration recovery results from Apple Sample.

Concentration Recovery Table	Spiked Concentration	Estimated Concentration from CDR
Test Dose 1	0.1 ppm	0.05 ppm
Test Dose 2	0.6 ppm	0.6 ppm

Table 4.3: Concentration recovery results for Strawberry Sample.

Concentration Recovery Table	Spiked Concentration	Estimated Concentration from CDR
Test Dose 1	0.1 ppm	0.06 ppm
Test Dose 2	0.5 ppm	0.5 ppm

Table 4.4: Concentration recovery results for Bell Pepper Sample

Concentration Recovery Table	Spiked Concentration	Estimated Concentration from CDR
Test Dose 1	0.05 ppm	0.03 ppm
Test Dose 2	0.5 ppm	0.4 ppm

Table 4.5: Concentration recovery results for Carrot sample

Concentration Recovery Table	Spiked Concentration	Estimated Concentration from CDR
Test Dose 1	1 ppm	1.3 ppm
Test Dose 2	10 ppm	12.4 ppm

4.6 Custom Electronics Platform

An integral part of the ElectrochemSENSE system is the custom electronic reader platform designed specifically to detect glyphosate pesticide in various samples by utilizing chronoamperometry as the electrochemical detection technique.

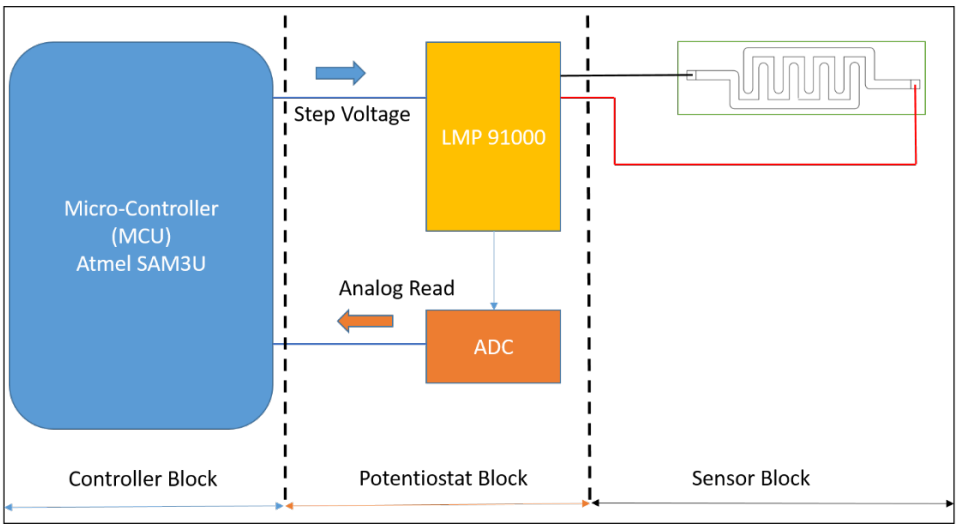

Figure 4.10: Block diagram to depict working function of ElectrochemSENSE Platform

For the Prototype Reader Instrument (as depicted in the functional diagram), an Atmel SAM3U (Microchip Technologies) was the microcontroller used and was interfaced with the ADC161S626 (Texas Instruments) micro-power ADC and the LMP91000 potentiostat IC (Texas Instruments). Working conditions for chronoamperometry was determined to be: Reference Voltage (Vref) of the system was maintained at 2.5V and the applied potential to the sensor was 20% of Vref (500mV) while Transimpedance Amplifier (TIA) Gain was kept at 35KOhm.

ADC circuit is capable of sampling at rate greater 50,000 samples/second while the required sampling frequency of interest is at 100 Hz. Hence, the designed system can clearly characterize the current peaks in CA measurement and used for our application.

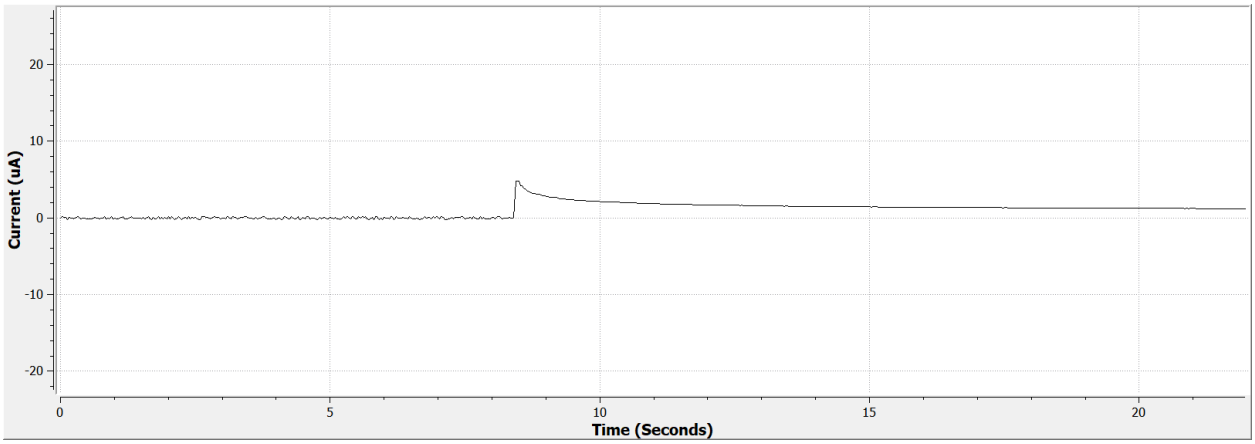

Figure 4.11: Sample Graph which shows CA measurement on prototype board as discussed above plotted using LMP91000 EVM software (Texas Instruments)

4.7 Study of Electrochemical Sensor Response in various Samples tested on ElectrochemSENSE device

The Purpose of this study is to characterize the performance results of the reader device. All the experiments (N=5) performed in section 4.5 is repeated in this section but instead of performing the tests on the Benchtop instrument (Gamry), all the experimental runs utilize the custom designed ElectrochemSENSE Platform.

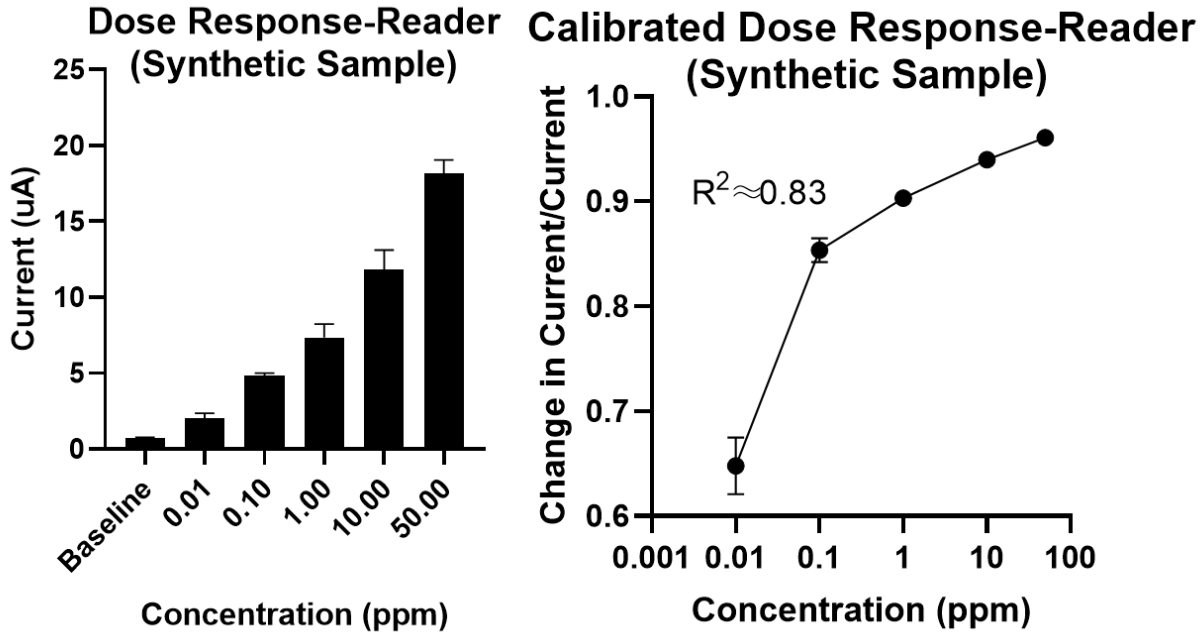

Figure 4.12: Dose Response and Calibrated Dose curve of Synthetic Sample measured with ElectrochemSENSE

Similar to the dose response observed for the synthetic sample measured using a benchtop potentiostat (Figure 4.6), In Figure 4.12 we find that, while a linear response of electrical signal with increase in concentration is visible from the CDR curve (plotted using current fraction calculated by equation 4), the sensor system approaches saturation around 10 ppm. This provoked a key inference that data from CDR combined with MRL data for each produce clearly highlights a Field Operating Range (FOR) (0.1 – 5 ppm), wherein the signal threshold is maximum.

Next, running the experiments similar to the conditions in section 4.5 on the ElectrochemSENSE device for the produce samples at low, MRL and high dose concentrations resulted in the dose response plot for all produce samples depicted in Figure 4.13 and the calibrated dose response (CDR) curve (Figure 4.14) extracted from it shows linearity with R^2=0.98 (averaged for all produce samples).

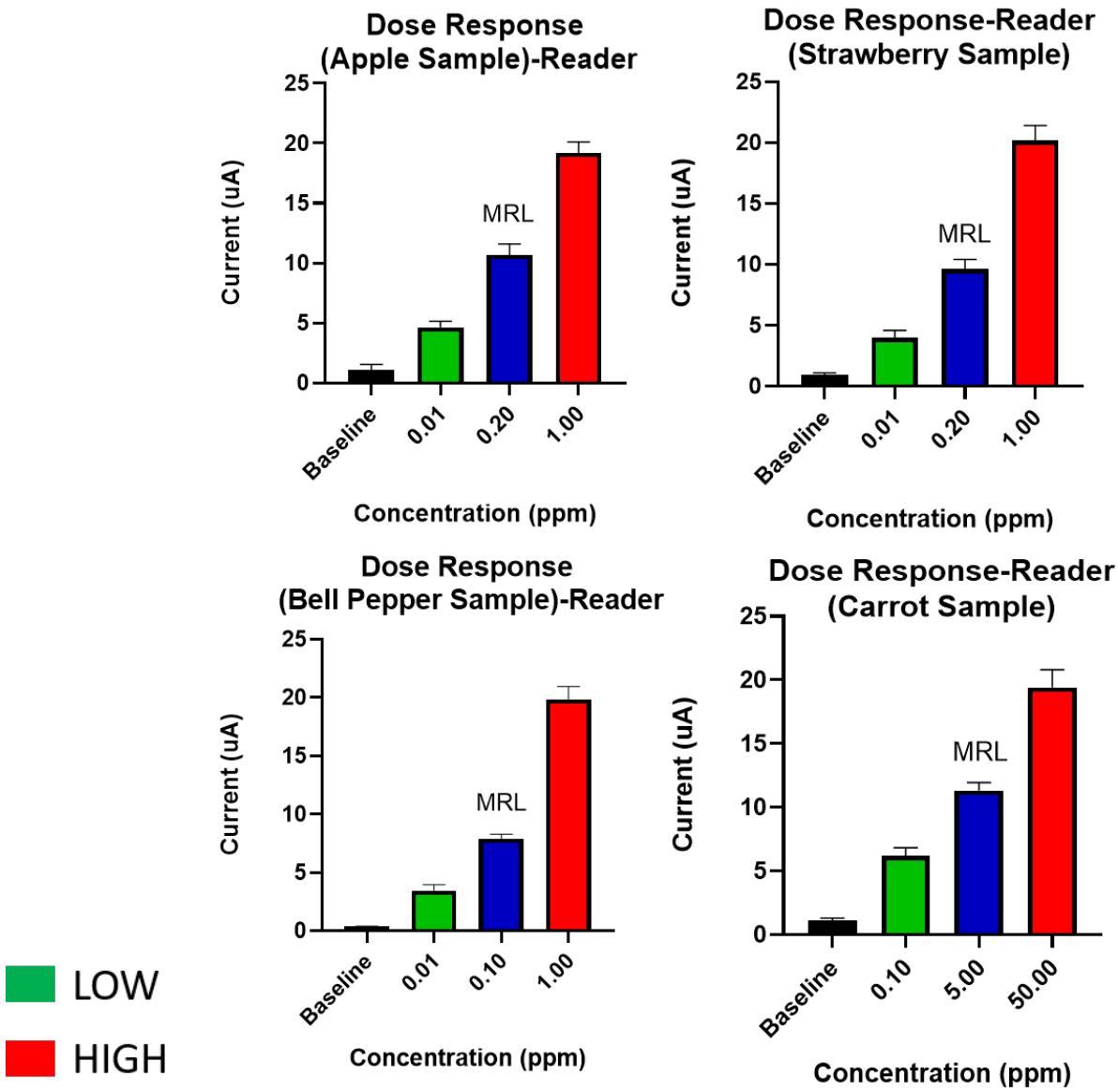

Figure 4.13: Dose Response of all produce samples (consolidated) measured with ElectrochemSENSE

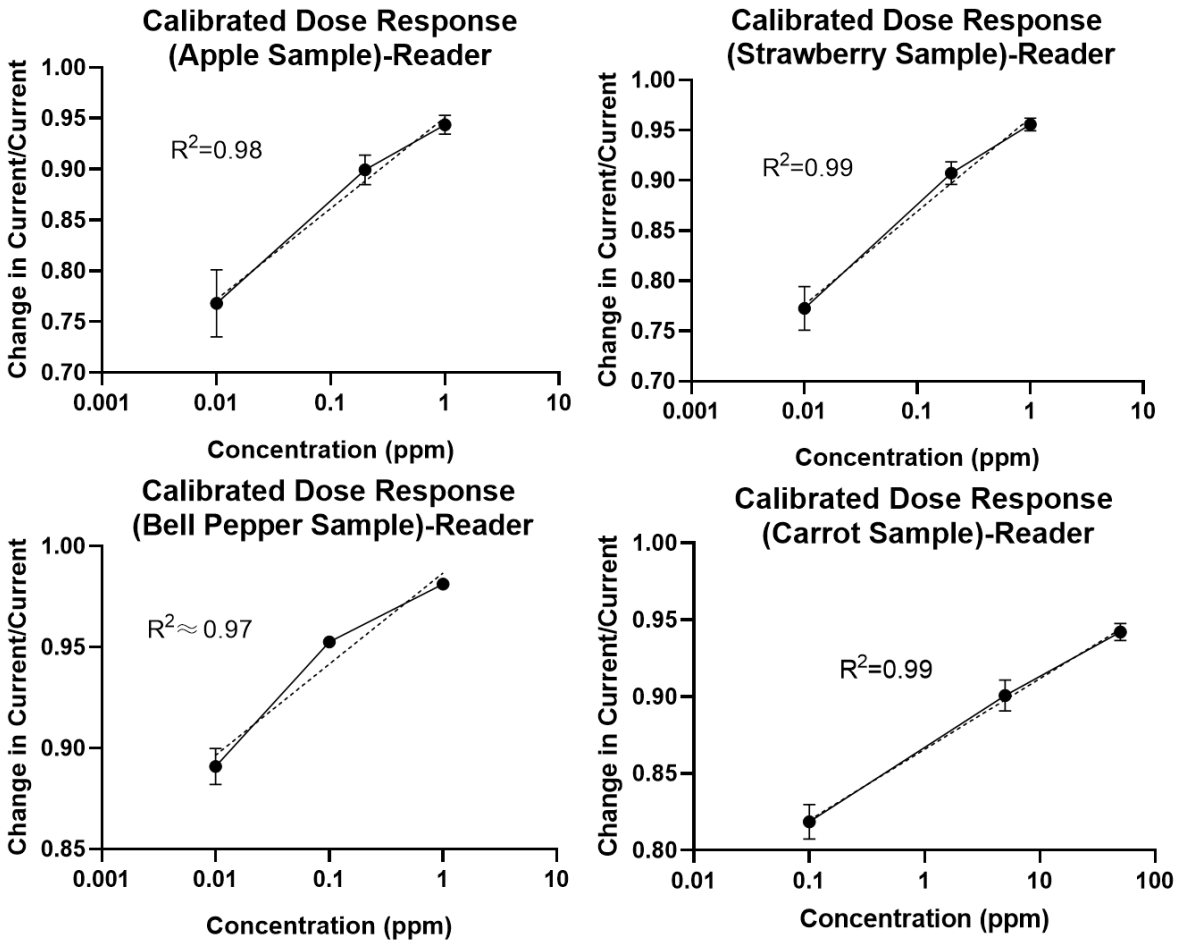

Figure 4.14: Calibrated dose response curve for all produce samples (consolidated) measured with ElectrochemSENSE

The Calibrated vs Test Response plot to determine whether the ElectrochemSENSE system can effectively detect random test samples is shown in Figure 4.15 and based on the results, it is gathered that although test doses could be detected based on the safety metrics for the produce given by the MRL database slight deviation from CDR was observed. Concentration recovery is again tabulated in order to quantify the extent of deviation as shown in Tables 9-12. Concentration recovery value is determined in a manner similar to the previous section.

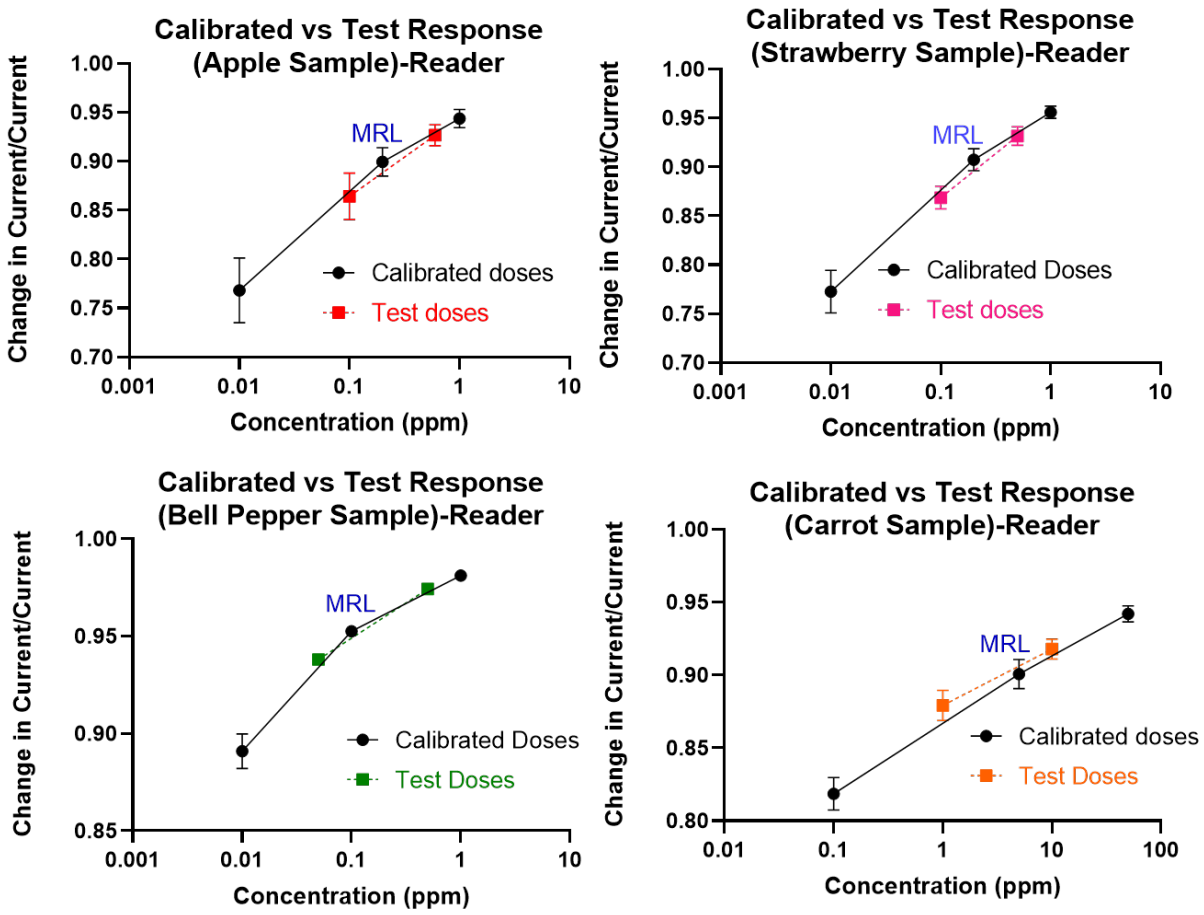

Figure 4.15: Calibrated vs Test Response graphs for all produce samples (consolidated) measured with ElectrochemSENSE

Table 4.6: Concentration recovery characteristics for Apple sample with ElectrochemSENSE

Concentration Recovery Table	Spiked Concentration	Estimated Concentration from CDR
Test Dose 1	0.1 ppm	0.1 ppm
Test Dose 2	0.6 ppm	0.6 ppm

Table 4.7: Concentration recovery characteristics for Strawberry sample with ElectrochemSENSE

Concentration Recovery Table	Spiked Concentration	Estimated Concentration from CDR
Test Dose 1	0.1 ppm	0.085 ppm
Test Dose 2	0.5 ppm	0.5 ppm

Table 4.8: Concentration recovery characteristics for Bell Pepper sample with ElectrochemSENSE

Concentration Recovery Table	Spiked Concentration	Estimated Concentration from CDR
Test Dose 1	0.05 ppm	0.06 ppm
Test Dose 2	0.5 ppm	0.5 ppm

Table 4.9: Concentration recovery characteristics for Carrot sample with ElectrochemSENSE

Concentration Recovery Table	Spiked Concentration	Estimated Concentration from CDR
Test Dose 1	1 ppm	1.5 ppm
Test Dose 2	10 ppm	12 ppm

4.8 Comparing the Two Measures: Potentiostat vs ElectrochemSENSE

One of specific aims of this research study is to determine the feasibility of ElectrochemSENSE as a sensitive sensing system that can be employed as a field test. Hence, the dose responses of the two measures were plotted in conjunction with each other to correlate both measures as shown in Figure 4.16.

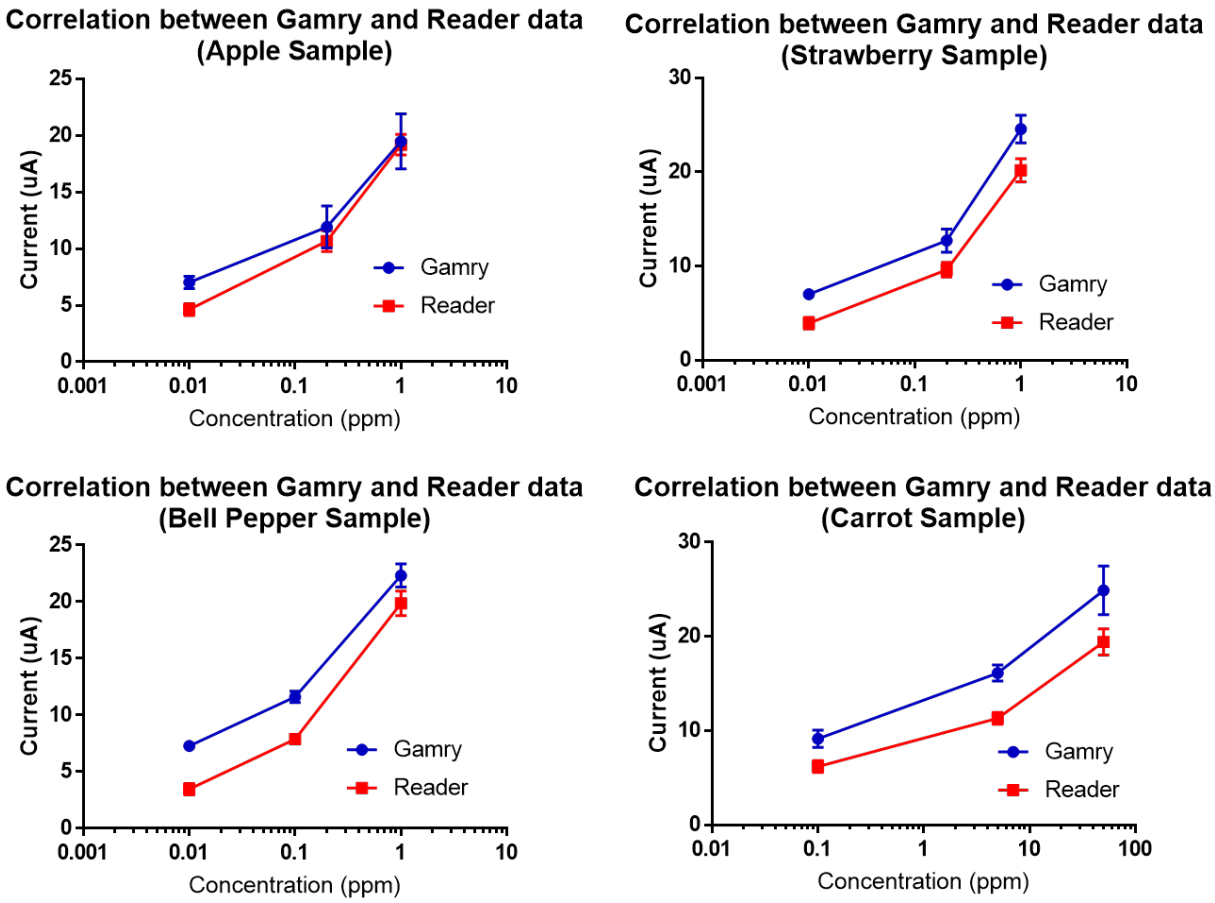

Figure 4.16: Dose responses of Potentiostat and ElectrochemSENSE instrument plotted together

It was noticed that with greater resolution of the electrical signal response, the magnitude was higher in the case of the lab benchtop instrument-Potentiostat than our designed reader-ElectrochemSENSE. However, from Figure 4.17- it is still clearly showcased that the signal

response of the handheld system is comparable to that of the benchtop model. This is enforced with the average Pearson's correlation coefficient greater than 0.99 indicating high correlation between the two measurement methods. Also, performing a t-test showed no significant difference between these two measures. Hence, it can be concluded that the handheld system is a feasible system to detect pesticide (Glyphosate) in produce.

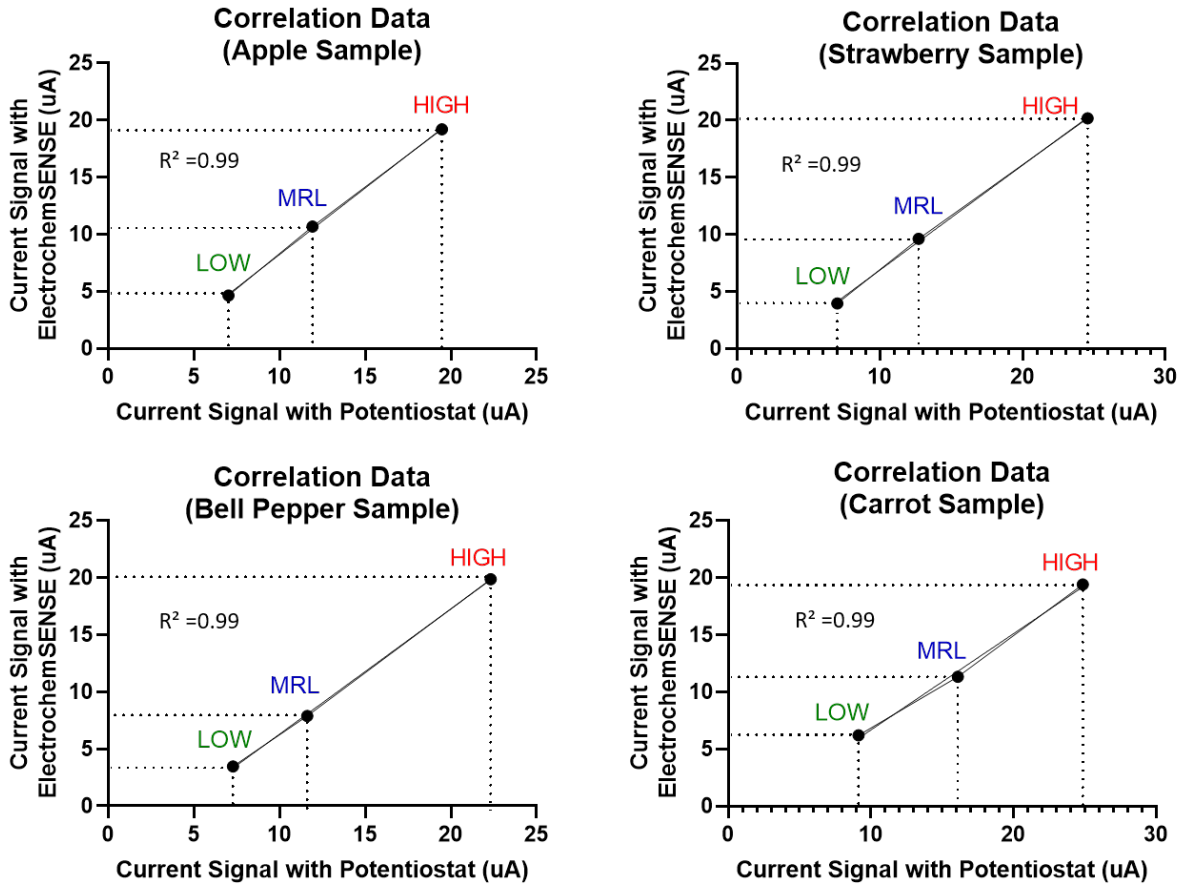

Figure 4.17: Current performances of Potentiostat plotted against that of ElectrochemSENSE

4.9 Machine Learning Classifier Integration

Integrating a machine learning model which serves as a classifier that can predict whether samples are safe or unsafe is an important analytics tool and tends to offer the ElectrochemSENSE system

better end to end functionality. For this study, MATLAB machine learning classifier application (in-built) was used as the ML tool to train the ElectrochemSENSE model and extract accuracy percentage for each sample set.

Based on training runs, support vector machine (SVM) and Bagged Trees algorithm were inferred as best suited for this application. Working of the algorithms are explained as follows:

4.9.1 Support Vector Machine (SVM) Algorithm [44]

Support vector machine is applicable for both regression and classification tasks, but more commonly used in classifiers. Overall objective of SVM is to identify a hyper plane in an N-dimensional space which does the function of clearly classifying the data points. Here, the 'N' represents the number of features based on the feature selection process. Hyperplanes can be defined as decision boundaries that are capable of classifying the data values in the system. Based on the side where the data lies with respect to the hyperplane, it can be attributed to different classes.

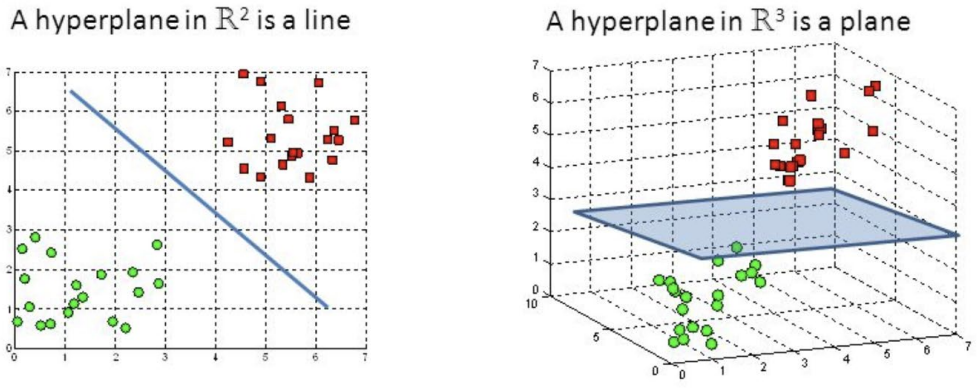

Figure 4.18: Representation of hyperplane with feature size N=2 (left) and N=3 (right)[44]

There can be many hyperplanes that can be chosen but for greater predictive capability, the hyperplane with the maximum margin (i.e.) hyperplane with maximum distance between data points of either class. This is so as to provide reinforcement so future data points can be classified with greater predictive confidence (accuracy). Support vectors are the data points close to the hyperplane and thereby affect the position and orientation of the plane, it is through these support vectors that the algorithm is capable of maximizing the classification margin.

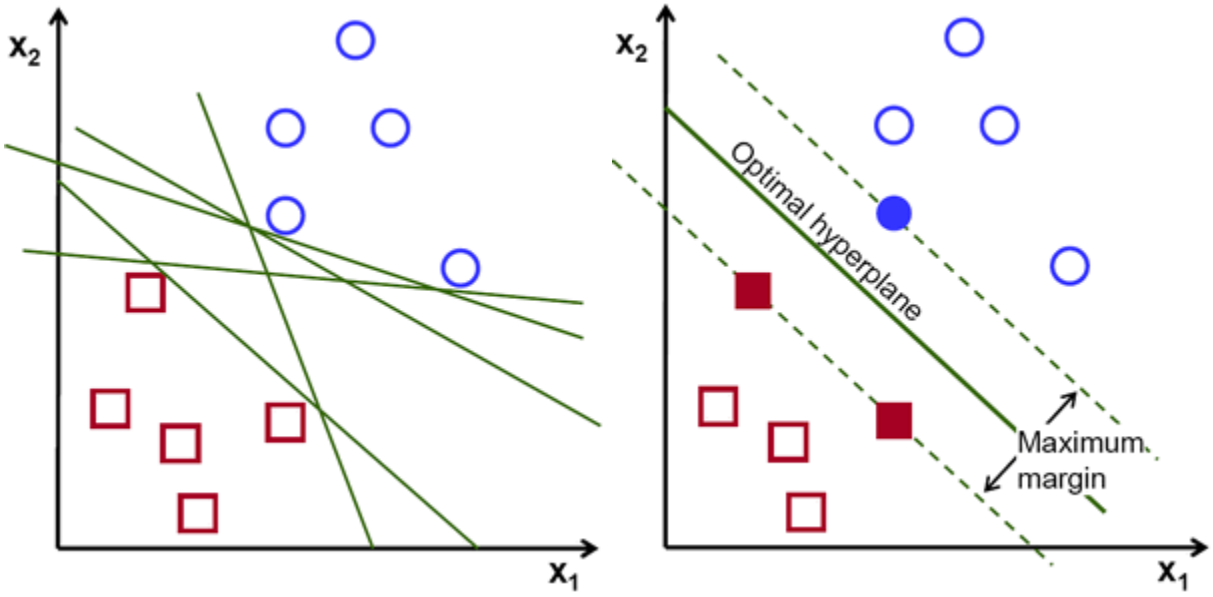

Figure 4.19: Various possiblities of hyperplanes available (left) and selection of optimal hyperplane with greater margin (right)[44]

4.9.2 Bagged Tree Algorithm (Decision Trees) [45] [46]

Bagged Tree is an algorithm which works based on the decision tree logic, it is most widely used in classification problems. 'Bagged' here means Bootstrap Aggregation wherein bootstrapping is a process of selecting random samples from a data set with replacement for estimating data set

statistics and model accuracy. Using this method, broadly, the population of the complete dataset is split or broken down into subpopulations based on significant splitters in the input variables (features).

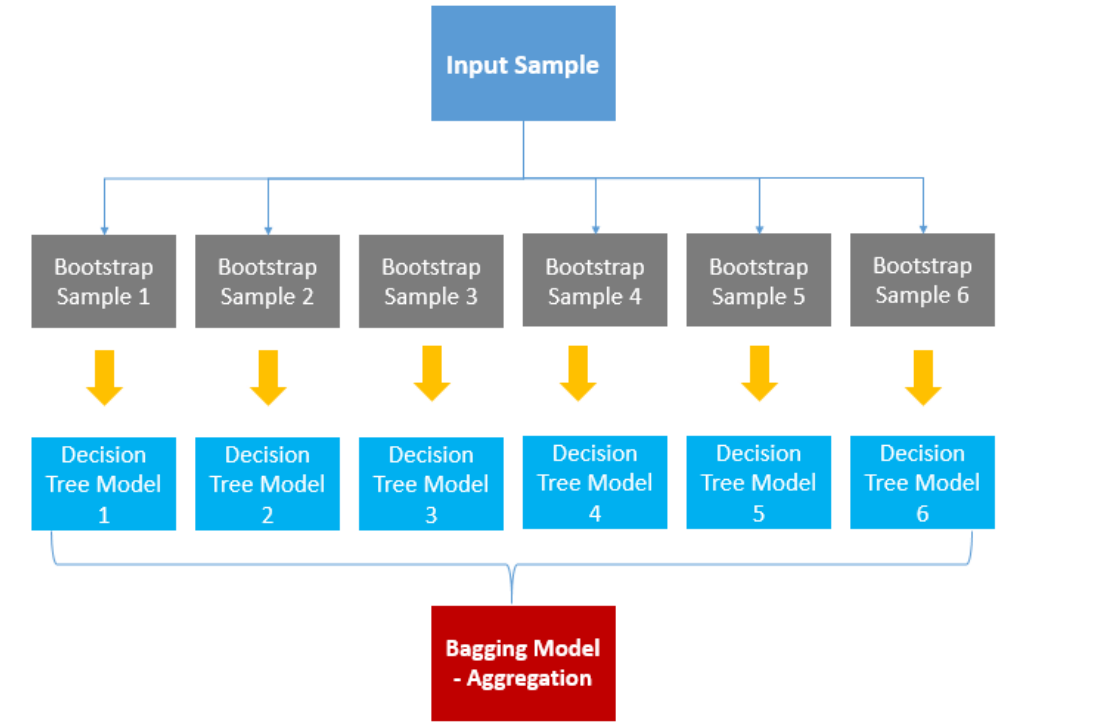

Figure 4.20: Block diagram representation of Bagged Tree Algorithm.[45]

Sub-population or node creation largely affects the accuracy of the decision tree, hence factors causing splitting of nodes is crucial in this algorithm. Objective is to create a homogeneous branching process i.e. decision trees splits nodes based on all variables and selects the split resulting in the most homogeneous tree system. This is implemented for multiple random samples from the whole dataset by bootstrapping method after which the results from each decision tree iteration is bagged (aggregated) together and a prediction response is given based on this aggregated model.

4.9.3 Training model

Integrating the classifier model to predict sensor performance is a key aspect of this study and is novel to the best of our findings. Certain key factors have been established prior to running the training protocol on MATLAB, this includes consolidating the data set in a manner so as to ensure easy feature extraction (Tableau workbook software tool was used for this aspect of the study), also the feature selection process was decided to utilize- dose represented in parts per million (ppm) and current values (Im) from the CA response corresponding to the dose as the input variables which forms either the support vectors in case of SVM or nodes in Bagged Tree. Further, based on these input variables, a conditional logic is applied based on MRL Concentration-(i.e.) if the corresponding dose concentration was equal to or lesser than the MRL value for that particular sample, then it is classified as SAFE with binary tag '0' while in the alternative case (>MRL) it is classified UNSAFE and binary value '1' associated to it. From this, the doses classified as safe or unsafe will be trained to predict the responses based on current values associated with each dose for each trial so the next time the system is exposed to a test case- it predicts the response from information in the trained dataset.

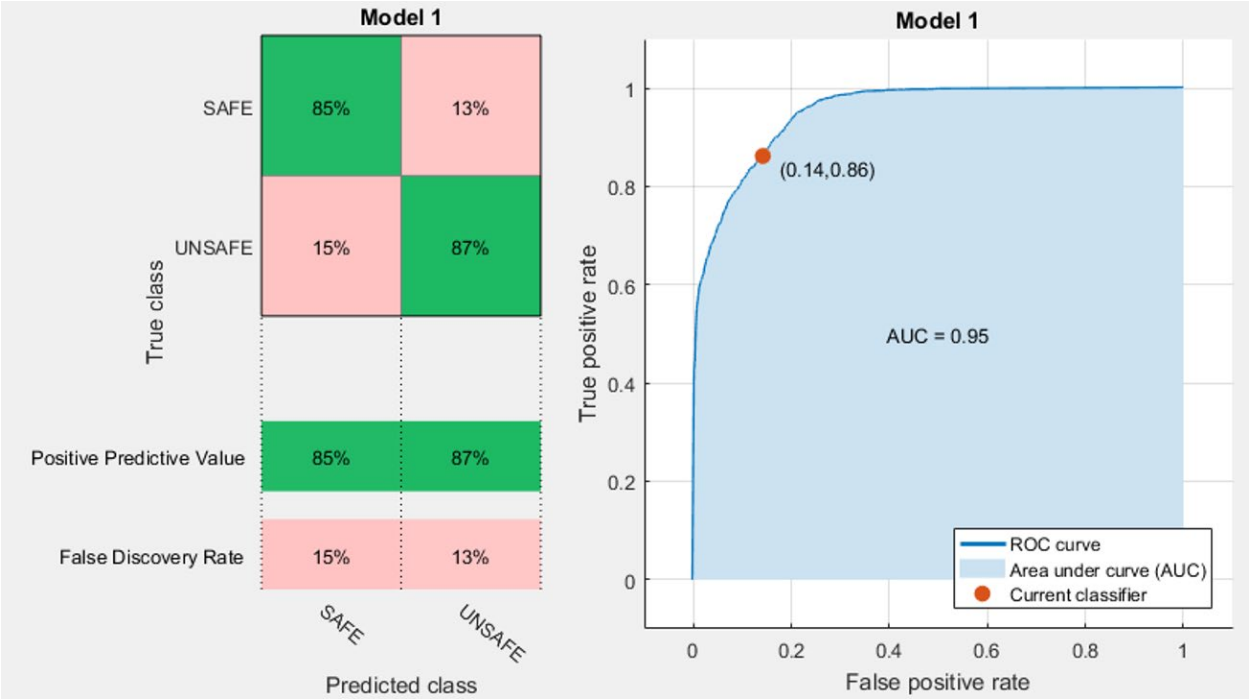

Figure 4.21: ML Training model performance in Synthetic Sample (PBS)

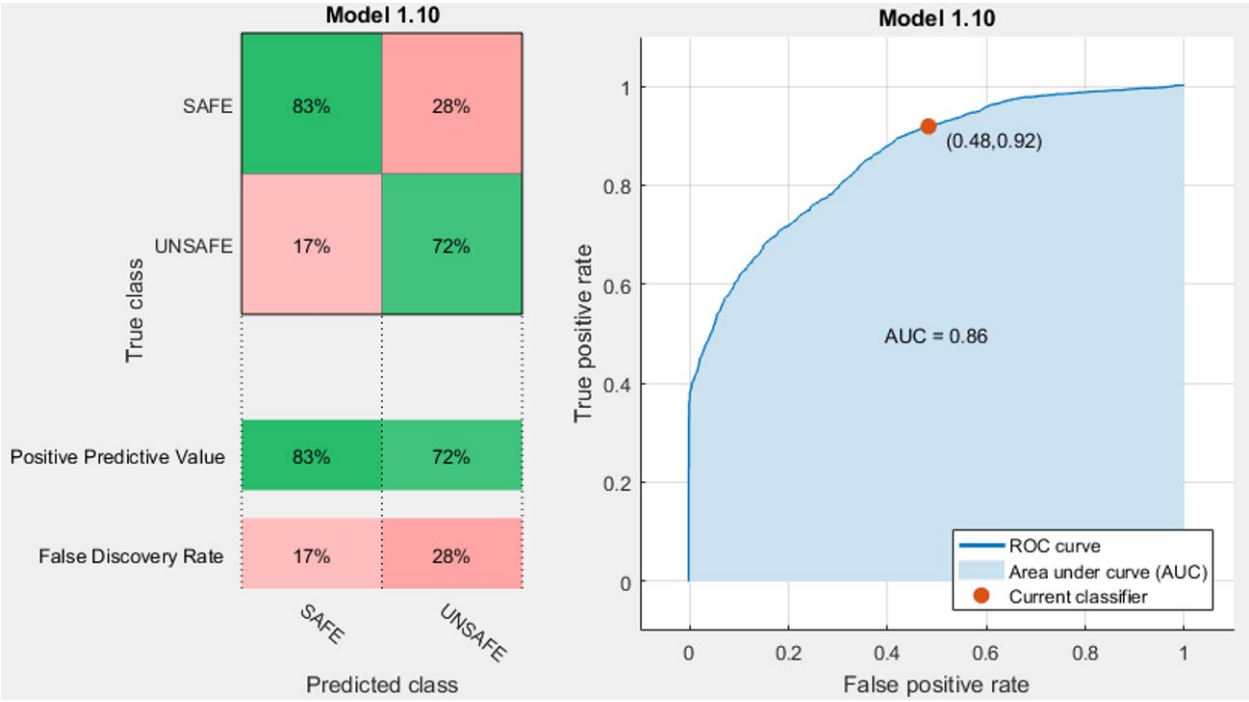

Figure 4.22: ML Training model performance in Apple Sample

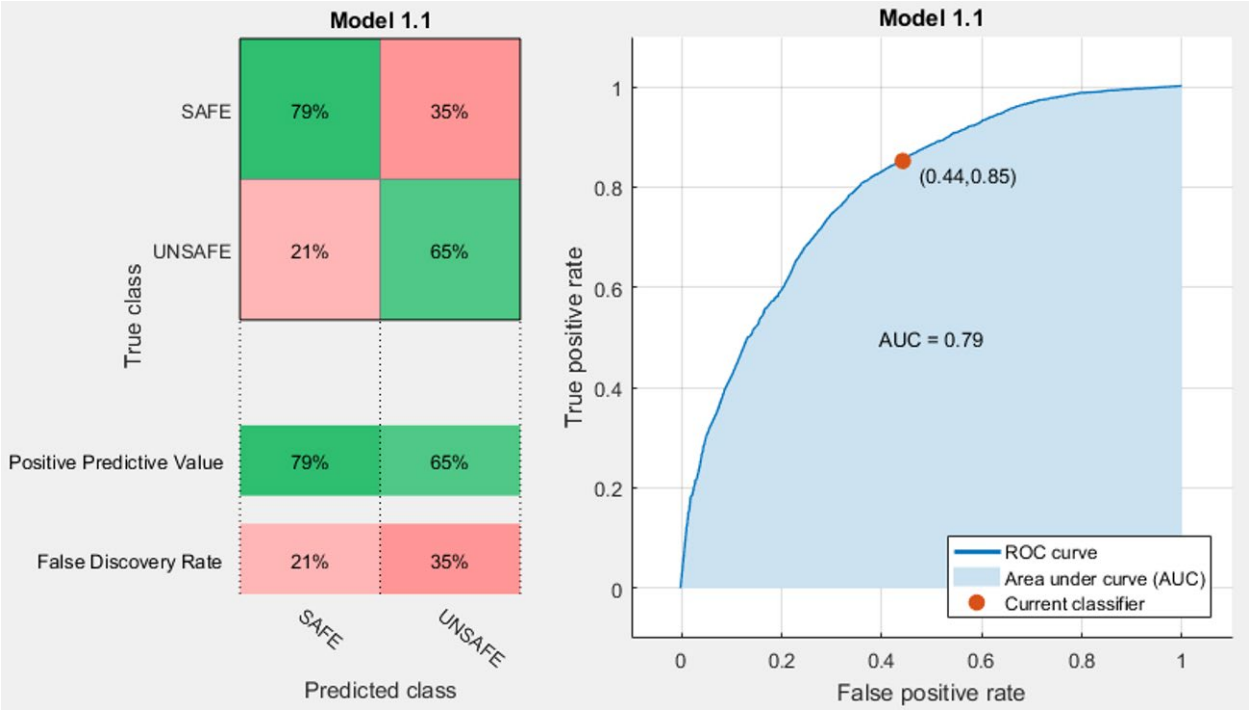

Figure 4.23: ML Training model performance in Strawberry Sample

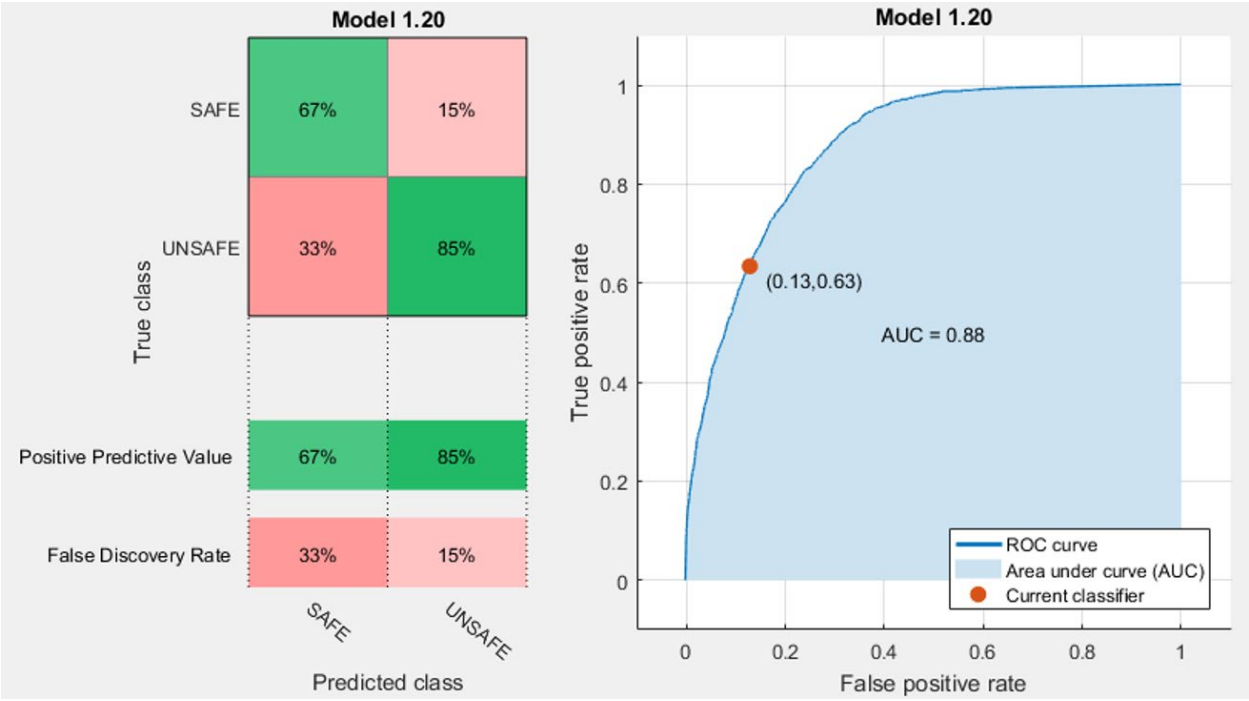

Figure 4.24: ML Training model performance in Bell Pepper Sample

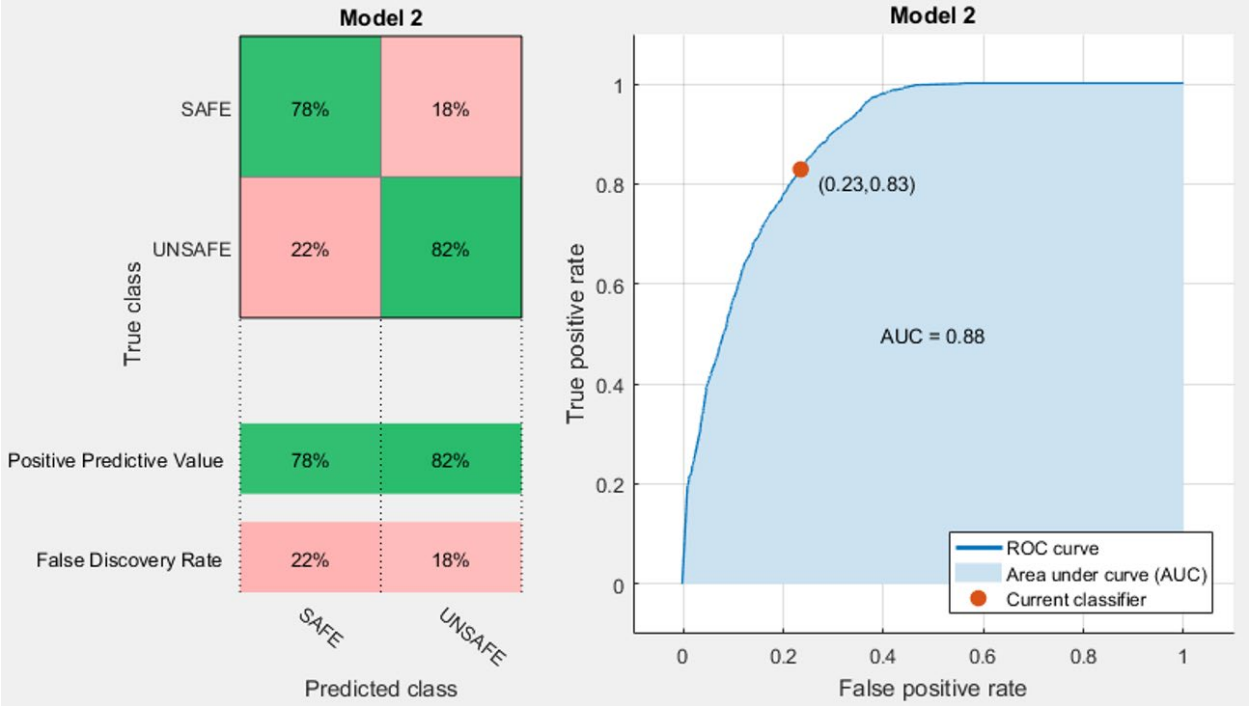

Figure 4.25: ML Training model performance in Carrot Sample

The results obtained by incorporating ML algorithm into the sensing system data as given above is for the data from various samples as seen in the experimental section is based on N=5 replicated each tested for 5 dose points. Accuracy was highest in the synthetic sample performance (Figure 4.21) with 86.4% followed by resultant metrics for apple and bell pepper with 80.3% and 80.2% respectively (Represented in Figure 4.22 and 4.24). Similarly prediction performances for strawberry (75.4%) and carrot (79.7%) samples are given by the data from Figures 4.23 and 4.25.

4.10 Cross-Reactivity Study

The goal of this experiment is to evaluate biosensor specificity towards glyphosate and also understand the effects of cross-reactive species or interferents towards signal response. It is important to study these characteristics as non-specific binding at the sensor interface causes variation in the signal response which could potentially lead to the formation of false positives. Sensor performance was tested on a similar pesticide of the same family (organophosphate)-Glufosinate. Chemical structures of glyphosate and Glufosinate are given in the Figure 4.26.

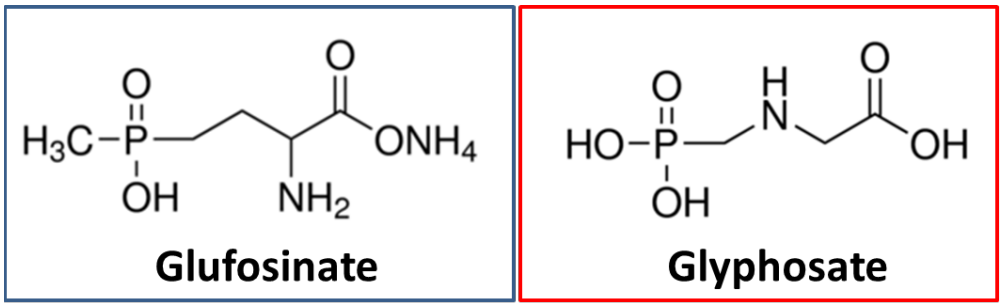

Figure 4.26: 2-D Chemical structure of Glufosinate[47] and Glyphosate[42]

The dose response for both antigens was quantified for N=5 sensor chips and plotted in Figure 4.27. Then, the current fraction is calculated and plotted against concentration (Figure 4.28).

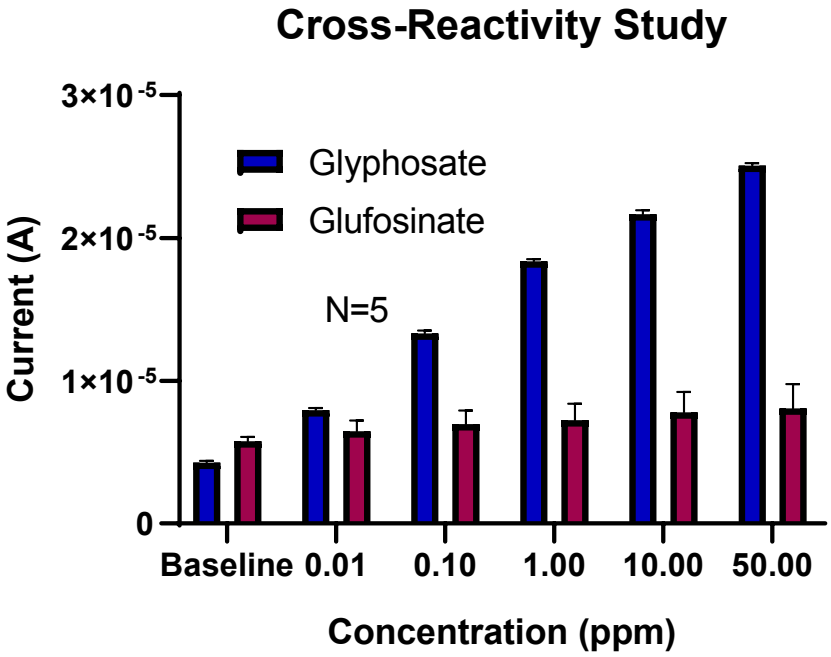

Figure 4.27: Dose Response of Glufosinate vs Glyphosate

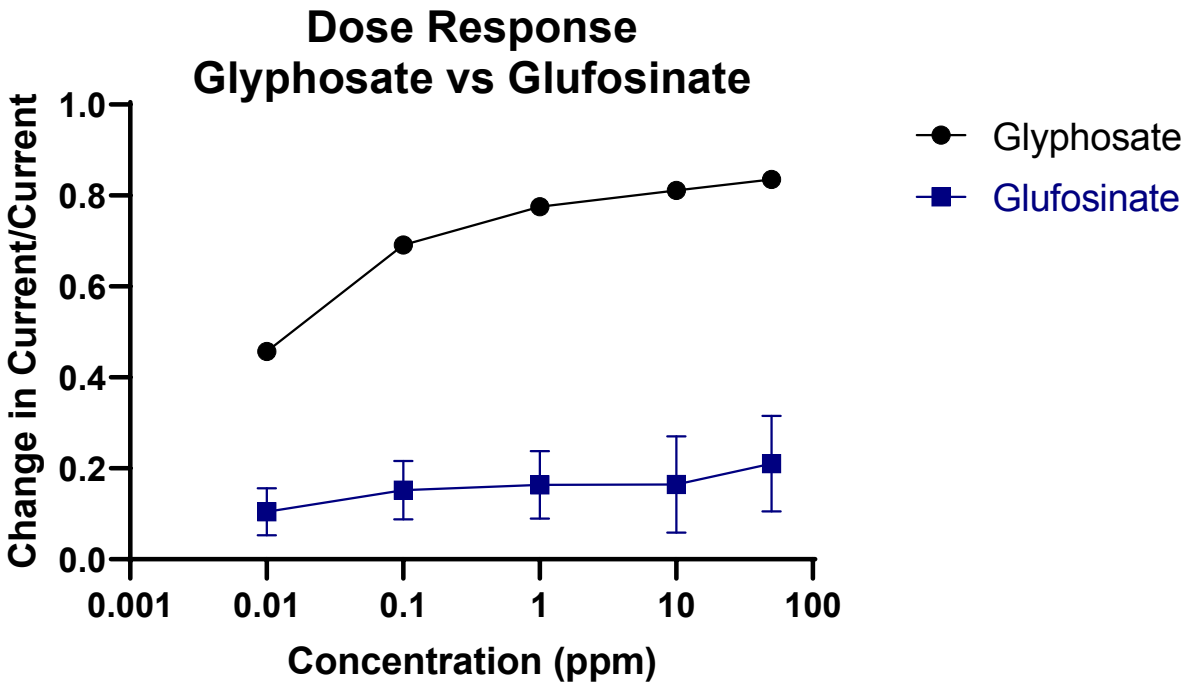

Figure 4.28: Cross-reactivity study response measured based on Current change

From Figure 4.28, we can see that with an increase in concentration of Glufosinate interferent-there is hardly any measurable change in current signal which is depicted as a near flat line (blue). Thus, it is enforced that the sensor and immunoassay is specific for glyphosate pesticide.

CHAPTER 5

FUTURE WORK

The immediate aim after validating system feasibility (i.e. proof of concept which is the current focus) is to further work on making the ElectrochemSENSE platform more sensitive and reliable and thereby, readily deployable for field use. This requires a lot more experimental runs to better calibrate the sensor response as well as integrate machine learning model completely (by training more sample sets) for predictive analysis in order to build an overall smart robust system. Next, Build a metric system (FOR) to sense and characterize pesticide levels in all vegetable and fruit produce (in addition to the 4 produce currently available). End goal is to build a multiplexed sensing system capable of detecting a spectrum of different pesticides.

CHAPTER 6

CONCLUSION

It has been shown that the proposed system offers real-time detection with response under 1 minute (< 60 seconds) while only using low sample volume of 5 μL to test for contamination with a Limit of Detection (LoD) of 0.01 ppm. Also, a new metric system for analysis has been devised in conjunction with MRL through Field Operating Range (FOR) determined for each produce type. Therefore, ElectrochemSENSE- A real-time, portable electrochemical sensing system in the form factor of a small hand held device has been shown to be viable for detecting glyphosate pesticide in various produce samples.

REFERENCES

[1] Pichetsurnthorn, P., Vattipalli, K. & Prasad, S. Nanoporous impedemetric biosensor for detection of trace atrazine from water samples. Biosensors & bioelectronics, ISSN: 1873-4235, Vol: 32, Issue: 1, Page: 155-62, 2012.

[2] Upasham, S., Tanak, A., Jagannath, B. & Prasad, S. Development of ultra-low volume, multi-bio fluid, cortisol sensing platform Sci. Rep. 8, 16745 (2018)

[3] Munje, R. D., Muthukumar, S., Jagannath, B. & Prasad, S. A new paradigm in sweat based wearable diagnostics biosensors using Room Temperature Ionic Liquids (RTILs). Sci. Rep. 7, 1950 (2017)

[4] Vasudevan, A., Prasad, S. "Sapsense"- Development of a Field Based Biosensor Towards Wheat Pathogen Detection, Page: 42-47 , 2017.

[5] A. Arul Selvi, M.A. Sreenivasa & H.K. Manonmani (2011) Enzyme-linked immunoassay for the detection of glyphosate in food samples using avian antibodies,Food and Agricultural Immunology, 22:3, 217-228.

[6] Ultrasensitive and Rapid-Response Sensor for the Electrochemical Detection of Antibiotic Residues within Meat Samples Hunter S. Stevenson, Shubrath S. Shetty, Noel J. Thomas, Vikram N. Dhamu, Ashlesha Bhide, and Shalini Prasad, ACS Omega 2019 4 (4), 6324-6330.

[7] Myers JP, Antoniou MN, Blumberg B, et al. Concerns over use of glyphosate-based herbicides and risks associated with exposures: a consensus statement. *Environ Health*. 2016;15:19. Published 2016 Feb 17. doi:10.1186/s12940-016-0117-0

[8] Andrea Houben; Eline Meulenberg; Theo Noij; Coen Gronert; Peter Stoks, Immuno affinity extraction of pesticides from surface water, Analytica Chimica Acta, ISSN: 0003-2670, Vol: 399, Issue: 1, Page: 69-74, 1999.

[9] Bettazzi, F.; Romero Natale, A.; Torres, E.; Palchetti, I. Glyphosate Determination by Coupling an Immuno-Magnetic Assay with Electrochemical Sensors. *Sensors* 2018, *18*, 2965.

[10] H. Stevenson, N. R. Shanmugam, A. P. Selvam, and S. Prasad, "The Anatomy of a Nonfaradaic Electrochemical Biosensor," SLAS Technol. Transl. Life Sci. Innov., vol. 23, no. 1, pp. 5–15, Nov. 2017.

[11] J. A. Nandhinee Radha Shanmugam, Sriram Muthukumar, Shajee Chaudhary and S. Prasad, "Ultrasensitive nanostructure sensor arrays on flexible substrates for multiplexed and simultaneous electrochemical detection of a panel of cardiac biomarkers," Biosens. Bioelectron., vol. 89, pp. 764–772, Mar. 2017.

[12] Kinnamon, D., Muthukumar, S., Panneer Selvam, A., & Prasad, S. (2018). Portable Chronic Alcohol Consumption Monitor in Human Sweat through Square-Wave Voltammetry. *SLAS TECHNOLOGY: Translating Life Sciences Innovation*, *23*(2), 144–153.

[13] de Araujo, J. S., Delgado, I. F., & Paumgartten, F. J. (2016). Glyphosate and adverse pregnancy outcomes, a systematic review of observational studies. BMC public health, 16, 472. doi:10.1186/s12889-016-3153-3

[14] Gasnier, Céline; Dumont, Coralie; Benachour, Nora; Clair, Emilie; Chagnon, Marie-Christine; Séralini, Gilles-Eric., Glyphosate-based herbicides are toxic and endocrine disruptors in human cell lines, Toxicology, ISSN: 1879-3185, Vol: 262, Issue: 3, Page: 184-91, 2009.

[15] Mesnage, R. et al. Multiomics reveal non-alcoholic fatty liver disease in rats following chronic exposure to an ultra-low dose of Roundup herbicide. Sci. Rep. 7, 39328; doi: 10.1038/srep39328 (2017).

[16] Nora Benachour and Gilles-Eric Séralini, Glyphosate Formulations Induce Apoptosis and Necrosis in Human Umbilical, Embryonic, and Placental Cells, Chemical Research in Toxicology 2009 22 (1), 97-105, DOI: 10.1021/tx800218n

[17] A. H.C. Van Bruggen; M. M. He; K. Shin; V. Mai; K. C. Jeong; J. G. Morris; M. R. Finckh., Environmental and health effects of the herbicide glyphosate, The Science of the total environment, ISSN: 1879-1026, Vol: 616-617, Page: 255-268, 2018.

[18] Sandrine P Claus, Hervé Guillou, Sandrine Ellero-Simatos., The gut microbiota: a major player in the toxicity of environmental pollutants? npj Biofilms and Microbiomes, Volume 2, 2016.

[19] Glyphosate: Health Concerns About the Most Widely Used Pesticide, USRTK, 2019.

[20] The Complete Guide to Roundup Exposure, Greenpal, 2018.

[21] Glyphosate, Dietary Exposure Analysis in Support of Registration Review, EPA, 2017.

[22] LC/MS/MS Method for Determination of Glyphosate, AMPA, and Glufosinate in Cereals, Olga I. Shimelis, Principal R&D Scientist, Reporter US Volume 34.4

[23] Angelika Steinborn, Lutz Alder, Britta Michalski, Paul Zomer, Paul Bendig, Sandra Aleson Martinez, Hans G. J. Mol, Thomas J. Class, and Nathalie Costa Pinheiro, Determination of Glyphosate Levels in Breast Milk Samples from Germany by LC-MS/MS and GC-MS/MS, Journal of Agricultural and Food Chemistry 2016 64 (6), 1414-1421, DOI: 10.1021/acs.jafc.5b05852.

[24] Fernando Rubio, Linda J. Veldhuis, B. Stephen Clegg, James R. Fleeker, J. Christopher Hall, Comparison of a Direct ELISA and an HPLC Method for Glyphosate Determinations in Water, Journal of Agricultural and Food Chemistry 2003 51 (3), 691-696, DOI: 10.1021/jf020761g

[25] Glyphosate Market for Conventional Crops and Genetically Modified Crop Applications: Global Market Perspective, Comprehensive Analysis and Forecast, 2017 – 2024

[26] Introduction to ELISA - Basics Guide, Bio-Rad.

[27] Enzyme-Linked Immunosorbent Assay (ELISA), Rockland antibodies and assays.

[28] Overview of ELISA, Thermo Fisher Scientific.

[29] Direct determination of glyphosate, glufosinate, and AMPA in soybean and corn by liquid chromatography/tandem mass spectrometry, Analytical and Bioanalytical Chemistry, 2016, Volume 408, Number 18, Page 4995, Narong Chamkasem, Tiffany Harmon.

[30] Noori, J. S., Dimaki, M., Mortensen, J., & Svendsen, W. E. (2018). Detection of Glyphosate in Drinking Water: A Fast and Direct Detection Method without Sample Pretreatment. Sensors (Basel, Switzerland), 18(9), 2961. doi:10.3390/s18092961

[31] Wikipedia contributors. (2019, April 9). Liquid chromatography–mass spectrometry. In Wikipedia, The Free Encyclopedia. Retrieved 14:34, April 29, 2019.

[32] Capillary Electrophoresis, Chemistry LibreTexts, 2019.

[33] Analysis of glyphosate, glufosinate and aminomethylphosphonic acid by capillary electrophoresis with indirect fluorescence detection, Sarah Y. Chang; Chia-Hung Liao, Journal of Chromatography A, ISSN: 0021-9673, Vol: 959, Issue: 1, Page: 309-315, 2002.

[34] Glyphosate ELISA kit assay protocol, Abnova.

[35] Glyphosate: mechanism of action, Glyphosate facts, Transparency on safety aspects and use of glyphosate-containing herbicides in Europe, 2013.

[36] Trends in glyphosate herbicide use in the United States and globally, Charles M. Benbrook, Environmental Sciences Europe, Bridging Science and Regulation at the Regional and European Level, 2016.

[37] Glyphosate fact sheet, NPIC.

[38] Harmful Pesticide Phaseout Calls Come as Some Countries' Use Rises, Bloomberg News, 2018.

[39] Glyphosate- tolerances for residues, Electronic Code of Federal Regulations, 2019.

[40] Structure of DSP (dithiobis(succinimidyl propionate)), Lomant's Reagent, Thermo Fisher Scientific.

[41] Glyphosate Toxicity – Government Approved Lies That Keep On Giving, Herb Scientist.

[42] Structure of Glyphosate, N-(Phosphonomethyl)glycine, Sigma Aldrich.

[43] The Biology Project: Immunology, Antibody Structure, University of Arizona, 2000.

[44] Support Vector Machine—Introduction to Machine Learning Algorithms, Towards Data Science, Rohith Gandhi, 2018.

[45] Bagging Algorithm: Concepts with Example, DNI Institute, 2016.

[46] A Complete Tutorial on Tree Based Modeling from Scratch (in R & Python), Analytics Vidhya, 2016.

[47] Structure of Glufosinate-ammonium, Sigma Aldrich.

[48] Deep dive into the science and history of Monsanto's glyphosate-based weed killer, Genetic Literacy Project, 2019

[49] Pesticides Industry Sales and Usage (2008 – 2012)- Market Estimates, EPA, 2017.

[50] National Center for Biotechnology Information. PubChem Database. Glyphosate, CID=3496, https://pubchem.ncbi.nlm.nih.gov/compound/3496.

[51] Which Current Distribution Interface Do I Use? COMSOL blog, Melanie Pfaffe, 2014.

BIOGRAPHICAL SKETCH

Vikram Narayanan Dhamu completed his Bachelor of Engineering degree in Electronics and Communication Engineering from Anna University, India, in May 2017. He joined the master's program in Biomedical Engineering at The University of Texas at Dallas in Fall'2017. In October 2017, he joined the Biomedical Microdevices and Nanotechnology Lab (BMNL) as a Graduate Student Researcher working under Dr. Shalini Prasad. He was invited to be part of the Honor society of Phi Kappa Phi –Chapter 316 for academic excellence in the year 2018. Currently, he has been working on building a smart bio-sensing platform, to develop a field deployable sensor device for environmental applications.

CURRICULUM VITAE

EDUCATION:

Masters of Science in Biomedical Engineering

The University of Texas at Dallas, USA (2017-2019*)

GPA: 4.00/4.00

Bachelor of Engineering in Electronics and Communication Engineering

Anna University, Chennai, India (2013-2017)

GPA: 7.33/10.00

RELATED COURSEWORK:

- Biomedical Microdevices, Nanotechnology and Sensors, Bioelectric Systems, Biomaterials and Medical Devices, Self-Assembly of Biomaterials, Image Guided Drug Delivery, Biomedical Image Processing, Genes, Proteins and Cell biology, Engineering Physiology of Human Body.

LAB EXPERIENCE:

Biomedical Microdevices and Nanotechnology Laboratory, UT Dallas (Oct 2017 – Present)

Principal Investigator: Dr. Shalini Prasad

MASTERS THESIS: **Portable Real-time Electrochemical Sensing System for the detection of Pesticide (2018-2019*)**

LAB SKILLS: Cleanroom fabrication, Wet Lab training, Laser Gravograph, 3D printing and modelling, Electrochemical Detection Techniques.

SOFTWARE SKILLS: Altium PCB Designer, AutoCAD, Arduino IDE, Inventor 3D, COMSOL Multiphysics, MATLAB.

AFFILIATIONS:

The Honor Society of Phi Kappa Phi – Chapter 316

Biomedical Engineering Society (BMES) - UT Dallas Chapter

Society for Lab Automation and Screening (SLAS)

PROJECTS:

1) Design of a Subcutaneous Microdevice in Cancer Theranostics.

- Electrochemical sensing system to detect specific breast cancer biomarker-tMUC1.
- Design of a triggered drug delivery mechanism to efficiently target estrogen receptors in breast tumor.

2) Analysis of Electrocardiographic waveforms of Mother and Fetus.

- MATLAB simulation to determine electrical correlation and distinction between maternal and fetal ECG data.

- Surveillance mechanism of the fetus vitals that can detect any ailments at an early onstage.

3) Photoacoustic mediated drug delivery of Raloxifene loaded Nano Cochleates in Breast Cancer Therapy.

- Use of photoacoustic imaging to mediate and deliver Raloxifene drug through nanocohleate carriers to tumor cells.
- High tumor specificity of the drug delivery method is hypothesized.

4) Teardown of Spirometry based sensor device.

- Evaluating/testing the sensor working principle and performance with PEF and FEV1 metrics.
- Design of an extrapolation model to correspondingly predict sensing function in the Nano realm and prove better efficacy.

5) Design of a novel Spinal cord Stimulation system.

- Problem study: Lead Migration, Breakage and infections in Spinal Cord Stimulation Systems.
- Proposed innovation: Alloy that is composed of platinum and titanium which is functionalized by bio-inert graphene using a polymer (polyethylene).

<u>UNDERGRADUATE THESIS:</u>

Design of a heart monitor using wearable electronics

- Wireless ECG monitoring system that can be purveyed via smartphone (Bluetooth) and can detect anomalies in heart waveform.

- Defibrillator build that can be controlled wirelessly using Bluetooth and behaves as an emergency medical wearable.
- Proposed to integrate the two systems to design an end to end (monitoring-diagnostic-stimulation) cardiac device.